NASA CR 120924
UM 026030-3-P

Annual Report

TWO PHASE DETONATION STUDIES CONDUCTED IN 1971

by

J. A. NICHOLLS

THE UNIVERSITY OF MICHIGAN
Department of Aerospace Engineering
Ann Arbor, Michigan 48104

prepared for

NATIONAL AERONAUTICS AND SPACE ADMINISTRATION

April 1972

Grant NGL 23-005-336

NASA Lewis Research Center
Cleveland, Ohio
R. J. Priem, Project Manager

1. Report No.	2. Government Accession No.	3. Recipient's Catalog No.
NASA CR 120924		

4. Title and Subtitle	5. Report Date
TWO PHASE DETONATION STUDIES CONDUCTED IN 1971	April 1972
	6. Performing Organization Code

7. Author(s)	8. Performing Organization Report No.
J. A. Nicholls	UM 026030-3-P
	10. Work Unit No.

9. Performing Organization Name and Address	11. Contract or Grant No.
The University of Michigan Department of Aerospace Engineering Gas Dynamics Laboratories Ann Arbor, Michigan 48105	NGL 23-005-336
	13. Type of Report and Period Covered Contractor Report

12. Sponsoring Agency Name and Address	14. Sponsoring Agency Code
National Aeronautics and Space Administration Washington, D. C. 20546	

15. Supplementary Notes

Project Manager, Richard J. Priem, Chemical Propulsion Division
NASA Lewis Research Center, Cleveland, Ohio

16. Abstract

This report represents an annual progress report describing, rather briefly, the research conducted on this grant. In those cases where the findings are already available in the open literature, the material is merely highlighted and appropriate references given.

There are five phases to the project which are described separately. The general subject matter of the phases includes:

1. Ignition of fuel drops by a shock wave and passage of a shock wave over a burning drop.
2. The energy release pattern of a two-phase detonation with controlled drop sizes.
3. The attenuation of shock and detonation waves passing over an acoustic liner.
4. Experimental and theoretical studies of film detonations.
5. A simplified analytical model of a rotating two-phase detonation wave in a rocket motor.

17. Key Words (Suggested by Author(s))	18. Distribution Statement
Detonation Shock Waves Droplet Combustion	Unclassified - unlimited

19. Security Classif. (of this report)	20. Security Classif. (of this page)	21. No. of Pages	22. Price*
Unclassified	Unclassified		5.50

* For sale by the National Technical Information Service, Springfield, Virginia 22151

FOREWORD

This report covers the progress made in the third year, February 1, 1971 to February 1, 1972, on NASA Grant NGL 23-005-336. The study was under the direction of Professor J. A. Nicholls, Department of Aerospace Engineering; Dr. R. J. Priem, NASA Lewis Research Center, was technical monitor.

Active participants on this program in the past year include:

Dr. C. W. Kauffman, former Ph. D. Candidate - Section II. A
K. Olzmann, Graduate Student - Section II. A
Hiroshi Miyajima, Visiting Researcher from Japan - Section II. A
T. Pierce, Ph. D. Candidate - Section II. B
R. Robidoux, Graduate Student - Section II. B
S. Prakash, Ph. D. Candidate - Section II. C
Prof. M. Sichel - Section II. D
Dr. C. S. R. Rao, former Ph. D. Candidate - Section II. D
Prof. T. C. Adamson, Jr. - Section II. E
Dr. P. Shen, former Ph. D. Candidate - Section II. E

TABLE OF CONTENTS

LIST OF FIGURES

ABSTRACT

This report represents an annual progress report describing, rather briefly, the research conducted on this grant. In those cases where the findings are already available in the open literature, the material is merely highlighted and appropriate references given.

There are five phases to the project which are described separately. The general subject matter of the phases includes:

1. Ignition of fuel drops by a shock wave and passage of a shock wave over a burning drop.
2. The energy release pattern of a two-phase detonation with controlled drop sizes.
3. The attenuation of shock and detonation waves passing over an acoustic liner.
4. Experimental and theoretical studies of film detonations.
5. A simplified analytical model of a rotating two-phase detonation wave in a rocket motor

I. INTRODUCTION

The research covered by this third annual progress report represents a continuation of our efforts devoted to the study of detonation waves in liquid-gas systems. The motivation for the work is associated with liquid propellant rocket motor combustion instability although certainly the studies are also applicable to internal combustion engines, jet propulsion engines, safety aspects of spilled liquid fuel, coal mine explosions, and weaponry. The research has been divided into 5 phases, although all of them are intimately related. For the most part these phases are briefly summarized and the reader is referred to other publications for a more complete treatment. The exception to this is where the material herein represents the only printed information available on the particular facet of the problem.

Phase A has been primarily concerned with the breakup and ignition of fuel drops by shock waves. The experimental portion of this study as well as a theoretical treatment of the ignition behavior was completed in the past year. The research is now concentrating on the passage of a shock wave over a burning drop.

Phase B has been devoted to the assessment of the approximate energy release pattern in two phase detonations insofar as they affect the significant overpressures observed.

Emphasis has been placed on detecting the variations observed when 2 discrete drop sizes, as compared to a monodisperse system, are utilized. Attention has also been given to an analytical prediction of the overpressures which, along with the experimental results, should yield the major energy release pattern.

Phase C has been aimed at the feasibility of arresting two phase detonations or the development of shock waves into a detonation by means of an acoustic liner. The engine case with a rotating detonation wave as well as a shock tube configuration have been considered.

Phase D has been concerned with film detonations, that is where the liquid fuel is in the form of a thin film on the wall of a tube. The experimental work and the two dimensional analysis were completed. The effort on this phase is now limited to preparing a NASA report on the subject.

Phase E consists of an analytical study of a rotating two phase detonation wave in an annular rocket motor. This problem has been essentially completed although a modest effort to include the radial effects is underway.

The progress made on each of the 5 phases will now be described.

II. RESEARCH RESULTS

Phase A - Shock Wave Ignition of Fuel Drops

Predictions of Wake Characteristics at Ignition.

Earlier in the program a number of experiments were performed wherein shock waves of varying strength were passed over liquid fuel drops in oxidizing as well as inert gaseous atmospheres. The aerodynamic shattering and ignition characteristics for diethylcyclohexane and n-hexadecane drops in oxygen and oxygen-nitrogen mixtures were determined for varying incident Mach numbers, different ambient pressures, and for differing initial drop diameters. Immediately after collision of the shock with the drop, liquid fuel, in the form of very small drops, is carried into the turbulent wake of the parent drop. Here the droplets vaporize and mix with the surrounding gases. After an ignition delay time, provided conditions are sufficient, ignition will occur in the wake. Experimentally it has been found that the ignition delay time depends on the fuel, initial drop diameter, the Mach number of the incident shock, and the initial oxidizer partial pressure. The significance of the Mach number dependence is primarily associated with the fact that the shock Mach number determines the dynamic pressure and temperature of the convective flow over the drop. The results of these experimental investigations are reported in detail in references 1, 2, and 3.

In order to gather some information on the conditions required in the wake of the drop before ignition could occur, an analysis was conducted which utilized some experimental information. This analysis is described in detail by Kauffman[3]. For the purpose at hand the analysis will just be outlined and a few representative results shown. First of all the analysis assumes a single drop and utilizes experimental results to describe the trajectory of this parent drop. The convective flow behind the shock and relative to the drop is then used in a boundary layer stripping model to calculate the size and rate of addition of microspray droplets to the wake region. The predicted variation of miscrospray drop size with time as the parent drop flattens transverse to the gas flow and breaks up is shown in Fig. 1. As indicated on the figure, the results are shown for a 1520μ diethylcyclohexane drop exposed to a Mach 3.75 shock in 20 in. Hg of pure oxygen. The predicted microspray drop sizes are small. Further, the analysis predicts that this size varies with the square root of the parent drop diameter. It is realized that the boundary layer stripping model used is not necessarily the dominant mechanism throughout the entire breakup history, particularly in the later stages. However, it was considered adequate for the purpose at hand and was used for lack of anything better. The variation of the peak micromist size for a range of shock strengths and initial pressures is shown in

Fig. 2. The decrease in size with M_S and/or with increased initial pressure is primarily due to the importance of dynamic pressure.

Combining the foregoing with the experimental observation that the microspray drops are almost instantaneously accelerated to the local gas velocity, the rate of evaporation of these drops at the local static pressure and temperature was calculated (admitting that the appropriate equation is not known for such dynamic conditions and under the influence of surface tension). As a result of all of the mechanisms involved , the composition of the wake will not be uniform in distance downstream of the parent drop. A calculation of such a variation is shown in Fig. 3 wherein the vaporized fuel-oxidizer ratio is shown as a function of distance behind the forward stagnation point of the parent drop. The variations for different times are shown for a 1520μ DECH drop upon interaction with an M = 3. 50 shock wave in 20 in, H_g of O_2. The experimentally observed ignition time was 77 μs. The stoichoimetric f/o ratio is 0. 292 by mass so that the maximum f/o ratio achieved in the wake is approximately 1/3 stoichiometric.

The lack of detailed knowledge of the kinetics of DECH oxidation has precluded the attainment of an ignition criteria derived from first principles. Accordingly, it has been necessary to examine the calculated state of the wake at the experimentally determined time of ignition; as was just done in Fig. 3.

The calculated total mass of fuel in the vapor phase in the wake

at ignition for a 1520μ drop subjected to various strength shocks at 3 different initial pressures is shown in Fig. 4. The plot indicates that for the reduced pressures of oxygen appreciably richer f/o ratios are required for ignition at any of the Mach numbers calculated and for reduced Mach numbers at a fixed pressure. The latter characteristic is presumably a temperature effect. However, the one atmosphere case showed essentially no variation with M_S. Similar plots made for other drop sizes indicate that more fuel vapor is in the wake at the onset of ignition for the larger drop sizes. This is borne out by the experimental observation that stronger blast waves are experienced with the larger fuel drops.

Finally, it is of interest to examine the sensitivity of the results to the uncertainty in the micromist size. Fig. 5 shows the variation of the maximum value of f/o in the wake at ignition for various shock Mach numbers and for the microspray drop size taken at 1/2, 1.0, and 2.0 times the liquid boundary layer thickness. The range extends over an equivalence ratio of about 1/8 - 2. While this spread is appreciable, it is encouraging that the predictions are at least reasonable.

Interaction of a Shock Wave with a Burning Drop.

The foregoing has been concerned with the ignition of a fuel drop by a shock wave. However, in actual combustion devices fuel drops are often burning before interaction with a pressure pulse.

Accordingly, an experimental study of the interaction of a shock wave with an initially burning fuel drop has been started.

The primary objective of this phase of the study is to determine the alteration of burning rate of the drop when exposed to a step pressure increase.

The apparatus which injects and ignites a single fuel drop into the shock tube is described in this section with some of the preliminary results of shock-drop interaction experiment.

The method of ignited drop injection is based on the sudden retraction of the assembly of a hypodermic needle, from which the drop is initially suspended, and an electrode, which gives an electric spark, shortly before ignition. The drop injection system is shown in Fig. 6. It essentially consists of a needle-electrode assembly and spring loaded plunger which is locked by the locking pin prior to the run. The solenoid retracts the pin and the plunger pulls up the needle-electrode assembly by a thin steel wire. The timing for activating the solenoid and spark electrode is accomplished by the shock wave through a pressure switch which is located 8.052 ft. upstream of the drop injection point. The ignition spark goes before the solenoid unlocks the spring loaded plunger, although the same signal from the pressure switch is used. The drop injection system is covered by a dome to facilitate evacuation and filling of the shock tube.

There are two major difficulties with this drop injection system which are not yet completely solved. First, the attainment of a single spherical droplet is difficult and secondly, there are certain technical limits in shortening the time interval between shock wave sensing and complete retraction of the needle-electrode assembly out of the shock tube.

The needle is made from a 0.035 in. o.d. x 0.022 in. i.d. tube with a 0.020 in. o.d. tube fitted inside.

Fig. 7 shows drops obtained from this system (non ignited, numbers indicate the time elapsed from the instant of short circuiting the pressure switch). During many trials to get acceptable shape of the drops, the following observations were made:

(a) The quantity of the fuel suspended before retraction should be a maximum. If the quantity of the fuel suspended is too small, the drop shape is distorted.

(b) The lateral movement of the needle during retraction should be minimized; otherwise, the drop is thrown laterally, distorted, and sometimes disintegrated into small droplets. Fig. 7 shows a little lateral movement of the needle in spite of considerable efforts to eliminate it.

(c) The suspended drop is distorted by the surface tension force when the needle is suddenly retracted. This makes the shape of the injected drop like a tadpole.

In hopes of eliminating the tail of the "tadpole", steps are being taken to minimize the opening of the fuel flow area at the needle tip. The use of a smaller diameter needle is also planned for obtaining more spherically shaped drops.

The time interval allowed between the instant of switching by the shock wave and the instant of shock wave-drop interaction is extremely small. For instance, at shock Mach number $M_S = 2.0$, the time interval is 3750 μs and at $M_S = 3.0$, 2500 μs. It is found that the major sources of prolonging retraction of the needle-electrode assembly are the current rise time of the solenoid and associated movement of the locking pin and the acceleration of the mass of the plunger and the needle-electrode assembly. The solenoid, which is rated at 24 VDC, is operated by a high voltage, short duration current discharge from condensers. Earlier, the condensers were charged to 320 V and the unlocking time was about 1800 μs. This time decreased to 1300 μs when the voltage was increased to 580 V. The unlocking time is determined from a discontinuity in the current-time trace from the oscilloscope.

The sum of the mass of needle-electrode assembly and plunger is about 15 grams. The spring constant of the spring used is 0.49 kg/cm and the initial upward force to the plunger is 8.4 kg. Simple analysis of a spring and mass system is in good agreement with the experiment. Experiment and the analysis shows that it takes about 3500 μs

for the needle to travel 10 mm upward.

Since there are no obvious ways of modifying the present electro-mechanical system to appreciably shorten the time interval, efforts are being directed to activate the appropriate time delay units from the time of bursting of the shock tube diaphragm.

At the higher shock Mach numbers, the needle-electrode assembly is still in the shock tube at the time of shock arrival and is damaged. Some effort is being made to devise a suitable protection of the needle electrode assembly without causing unfavorable disturbance to the interaction phenomena.

A series of preliminary experiments using fairly weak shock has been made. Fig. 8 shows the sequence of pictures of interaction of an ignited drop with shock waves. Although the disturbance from droplet shape, i. e. from the tale of the "tadpole", is considerable, most of the features of interest of the interaction are retained. The shock Mach number is 1. 55 and the nominal drop diameter is 2040 μ. It is noted from Fig. 8 that the shock is accelerated drastically in the hot region. The initial laminar flame is blown off the drop by the convective flow behind the shock. The blown off flame apparently ignites the micromist in the wake region in between 50 to 70 μs after initial interaction. Fig. 9 shows the sequence of the interaction of a shock wave with a drop which has not been ignited. The break up characteristics are not noticeably different from those of the ignited

drop. However, it is seen from the comparison of Fig. 8 with Fig. 9, that the micromist in the wake region is consumed much more in the case of the initially ignited drop.

In these cases where the flame attaches to the wake, the subsequent shed micromist will be continously consumed and hence the severe blast wave phenomenon, experienced in shock wave ignition[1] will be precluded.

Accordingly, it is worth while to determine the condition under which the flame will remain attached to the drop, attached to the wake, or completely blown off. To this end, streak schlieren photography will be used in experiments utilizing various shock strengths and initial oxygen concentrations. The affect on burning rate will also be established.

Phase B - Energy Release Patterns

Four series of experimental tests were conducted subsequent to the previous report[4]. Two of these involved polydisperse spray detonations consisting of DECH as fuel in a pure gaseous oxygen environment, while the other two were concerned with the dilution of the charge gas with unreactive and reactive gaseous additives.

As was done previously, the composition of a polydisperse spray was described in terms of the total equivalence ratio, ϕ_T, and the partial equivalence ratios, ϕ_i, of the constituent drops, where $\phi_T = \sum_i \phi_i$. Also, the "equivalence ratio fraction" of species i is $a_i = \phi_i/\phi_T$.

In the first series of tests, sprays were detonated which consisted of 300μ and 1300μ diameter drops, with $a_{1300} = 0.525$ and $\phi_T = 0.80$. This bimodal distribution represents the maximum separation in drop sizes possible using the polydisperse drop generator[4], under the condition of approximately equal division in total available energy between the two species. A monodisperse spray of 1300μ diameter drops was detonated for comparison at $\phi_T = 0.80$, but the corresponding monodisperse spray of 300μ diameter drops could not be produced at this equivalence ratio, since 38 drop-producing cappilaries would have been required of the drop generator which has a 20-needle capacity.

The structural differences between the monodisperse (1300μ) spray and the bimodal (1300μ, 300μ) spray detonations can be observed in Fig. 10. The apparent ignition plane of the 1300μ drops (at about 2 in. behind the leading shock) is more distinct in the monodisperse than in the bimodal case. The intensity of the explosive ignition of the large drops has been somewhat subdued by the earlier ignition of the small drops. In addition, the mean pressure level is more sustained in the monodisperse than in the bimodal spray. This is because, in the bimodal spray, the small drops, once ignited, add energy in the region ahead of the large drop ignition plane, causing the pressure level there to drop; in the monodisperse spray of large drops, the pressure remains fairly constant until the drops ignite.

The average detonation velocity in a monodisperse spray of 1300μ drops at $\phi_T = 0.8$ was $U_s = 5220$ ft/sec while in the bimodal spray it was $U_s = 5890$ ft/sec, an increase of about 11%. This results in a lower average pressure in the monodisperse case (even though it is more sustained) by about 25%. It appears that with a large drop size difference in a polydisperse spray, the factor which most greatly influences the average pressure levels in the wave is the extent to which shifts in distribution affect wave velocity and the leading shock wave pressure. With lesser drop size differences, the wave velocity is not as greatly affected by distribution, and in that case, the average pressure levels appear to be related to distribution through the tendency towards increasingly sustained pressures as the proportion of large drops is increased.

Another series of experiments examined the effect of total equivalence ratio on detonation properties. Bimodal sprays of 300μ and 750μ diameter drops were used. The tests were conducted at constant equivalence-ratio fraction, $a_{750} = 0.550$, with total equivalence ratios varying between $\phi_T = 0.265$ and $\phi_T = 0.775$.

The decrease in droplet spacing accompanying an increasing ϕ_T was expected to result in progressively smoother energy release. That is, due to the increasingly probable proximity of small drops to the wakes of the large drops, the explosive ignition of the former could be expected to cause ignition in these wakes earlier than normal. This should result in a decrease in the intensity of large-drop blast waves.

The expected tendency of decreasing overpressure ratio with increasing ϕ_T was observed (Fig. 11). However, the pressure structure smoothness did not improve over the range of ϕ_T studied.

Although the peak overpressures in Fig. 11 are decreasing, the magnitude of the average reaction zone pressure increases with increasing ϕ_T (Fig. 12). This is due to increasing shock pressures resulting from an increasing total heat addition, which is also accompanied by an increasing wave velocity (Fig. 13).

The third series of tests dealt with the effect of charge gas dilution by nitrogen. Monodispersed DECH sprays consisting of 750μ diameter drops were employed in these experiments, with the charge gas mixtures at 1 atm pressure.

The equivalence ratio of DECH with respect to the oxygen present in the charge gas was held at $\phi_T = 0.914$ in all tests.

The detonation velocity as a function of nitrogen mole fraction, X_{N_2}, is plotted in Fig. 14. Nitrogen mole fraction is the ratio of the number of moles of nitrogen to the total number of moles of nitrogen and oxygen in the charge gas. The greatest N_2 content which produced detonation was $X_{N_2} = 0.5$. Prior to this point the detonation velocity appears to be only slightly affected by the presence of the N_2.

The average pressure level in these waves (Fig. 15) decreases significantly with increasing nitrogen concentration. This is due to a decreased intensity of the explosive ignitions by individual drops in the spray, which reduces the average overpressures. Peak overpressures were not as strongly affected by N_2 content.

When the diluting additive is a reactive gas, the detonation system is of mixed type, consisting of gas-phase and two-phase parts. These are referred to as "hybrid" detonations. In such detonation, the gas-phase reaction is presumably completed well before the drops ignite. Hence the equivalence ratio of the gas-phase component is defined in terms of the initial oxygen present. On the other hand, the equivalence ratio of the two-phase part may be expressed in terms of either the initial oxygen concentration, or the oxygen concentration remaining after completion of the gas-phase part. In the experiments

presently described, the equivalence ratio of the liquid fuel is measured with respect to the initial oxygen content. These tests were conducted in monodisperse sprays of 480μ diameter drops, with hydrogen gas as the diluent. The equivalence ratio of DECH was held at unity.

Wave velocity and Mach number as functions of hydrogen concentration are shown in Fig. 16, along with the corresponding gas-phase hydrogen-oxygen curves for comparison. At low hydrogen mole fractions, the two-phase detonation supports the H_2-0_2 reaction, whereas at high hydrogen concentrations, the H_2-0_2 detonation supports the two-phase part.

Very pronounced structural changes occur with increasing hydrogen content. These are shown on Fig. 17. The apparent ignition zone position of the liquid drops moves rearward in a continuous manner. Moreover, the addition of heat to the flow field in the region just behind the leading shock by the H_2-0_2 reaction produces progressively reduced overall reaction zone levels.

After X_{H_2} = 0.5, droplet ignition is so delayed that there exist in the records from these waves extended regions of relatively minor pressure excursions behind the leading shock and the voilently reacted liquid drops appear to act as a "piston" in preventing the trailing rarefaction behind the gas detonation. After X_{H_2} = .667 (stoichio-

metric), no overpressures appear, and the fuel from the liquid drops probably reacts much more gently.

Many of the resutls just described were presented in a paper entitled, "Two-Phase Detonations with Bimodal Drop Distributions," which was presented at Third International Colloquium on Gasdynamics of Explosions and Reactive Systems, Marseille, France. The paper has been accepted for publication in Astronautica Acta.

The theoretical description of the reaction zone structure in a monodisperse two-phase spray detonation has progressed. The ignition time estimates described previously[4] have been compared with revised experimental data (Fig. 18 and 19) showing improved correlation, particularly in the case of the "whole wake" thermal imbalance theory. This theory predicts the occurrence of explosive ignition when the rate of heat production due to pre-ignition reaction in the wake region of a given parent drop in the spray exceeds the rate of energy removal from this region due to turbulent mixing with the external stream.

A detailed analytical account of the time-varying processes which take place in the reaction zone of a two-phase detonation has been prepared in this analysis, each individual droplet in a fuel spray through which the detonation passes is presumed to undergo the sequence of events described by the "whole wake" ignition theory. The blast waves

produced by the individual wake explosions colalesce, after a certain distance, into two planar shocks, one of which moves towards the leading shock (forward-moving) and the other which moves away from it (rearward-moving).

The model is constructed in a one-dimensional coordinate system which moves at the average detonation velocity. Fuel droplets arranged in a square array pass through the leading shock, and after traveling a distance into the reaction zone corresponding to the overall ignition delay time, a given plane of drops ignites. The details of the three-dimensional process by means of which the individual spherical blast waves (from each drop in this plane) coalesce into planar waves is not analyzed. However, the time from ignition to coalescence, during which three-dimensional effects are important, is assumed to be negligibly small. The one-dimensional distributions of the gasdynamic variables within the blast wave region just after coalescence occurs is forced to satisfy integral conservation of mass, momentum, and energy with respect to that which existed in the same physical region just prior to ignition.

Thereafter, the one-dimensional blast wave is allowed to freely expand within the reaction zone. For this purpose, a two-step (predictor-corrector) numerical scheme[5] is utilized to solve the Navier-Stokes equations within the blast wave region.

Eventually, the forward-moving shock from the blast wave will

overtake the leading shock, imparting to it an increased velocity. This is the mechanism of wave sustenance; i. e., between successive collisions of this type, the leading shock decays. Hence the detonation does not actually propagate at a constant velocity, but oscillates about an average speed.

The detonation structure contains a timewise periodicity resulting from the regularly occurring explosive ignitions. The frequency of these ignitions is coupled to the average wave velocity and the spacing between the droplet planes. After each ignition, the newly formed blast wave itself expands within the expansion wave of its predecessor. Several such nested blast waves can be present within the reaction zone at a given instant.

Only a fraction of the total energy available in a drop is released when it ignites. A significant mass of fuel survives in the form of microspray and in the parent drop. Subsequent to ignition the drop-shattering and microspray evaporation processes continue, with the difference that it now occurs in a much hotter and more turbulent region.

For purposes of analysis, the post-ignition reaction process is decoupled from its complex aerothermodynamic interaction with the convective flow, and a simplified energy release rate is assumed. It is also assumed that the drops remain in their original orientations so that each plane of drops acts as a separate,

moving heat source within the flow in the reaction zone, downstream of the ignition point.

The results from this calculation are graphically displayed utilizing a high speed (1200 baud information exchange rate) Computek CRT terminal. Plots of pressure, density, temperature, and gas velocity are recorded as functions of position within the wave, at given times in the calculation. In addition, a computer-animated film follows the time-varying structure of the detonation through several cycles.

An example of the data generated by this calculation is presented in Fig. 20. The abscissa of the plot denotes distance from the explosion center; i. e., the position within the reaction zone at which the periodic explosive ignitions occur. In producing the movie, this plot would represent one image, of which four frames on the film would be taken.

When this calculation is completed on a given set of conditions, there is effectively available a field of data in the x-t plane (within limits on x and t) within which all information is known, including the shock positions and strengths and the values of the gasdynamic variables between shocks. Therefore, additional information can be gained by simulating the movement of a pressure transducer through this field.

In leading shock fixed coordinates, such a transducer penetrates the reaction zone along a path in the x-t plane described by $dx/dt = U_s$ (the detonation velocity). At any given instant, the output from the transducer represents an integration of the pressure distribution over its exposed surface.

For a circular transducer of 0.1 in. diameter, a typical transducer "sweep" of this type (through the data from which Fig 20 was taken) is shown on Fig. 21. The abscissa is now transducer distance behind the leading shock.

It can be seen that the shocks appear to the transducer as rounded "bumps". There is also a rise time even at the leading shock, corresponding to the time of leading shock passage over the transducer.

The one dimensional-time unsteady-structure of a two phase detonation just described will be presented in a paper for the forthcoming 14th International Symposium on Combustion, The Combustion Institute, Pennsylvania State University, August 1972.

A detailed coverage of all of the material of this Phase B will appear shortly in the Ph. D. thesis of T. H. Pierce.

Phase C - Acoustic Liner Studies

The study of the effectiveness of acoustic liners as attenuation devices for two-phase detonation waves has been the principal aim for this phase of our work. Fully recognizing that to be effective the acoustic liner has to damp out compression waves generated in the combustion zone and thereby hopefully preclude the development of the combustion (or flame) front into a detonation, different aspects of the interaction of shock waves and detonation waves with acoustic liners have been studied. So far the limited experimental observations and the approximate analytical calculations have indicated that for relatively weak shocks of strength comparable to the pressure pulses in the combustion zone the shock velocity reduction obtainable by interaction with an acoustic liner is relatively small[6,7]. The mass efflux from behind the shock wave into the liner cavities appears to be the main cause of the velocity change in the shock wave.

An analysis to study the effect of mass bleed behind the leading shock of a two phase detonation wave has been completed. Jump conditions for a two phase mixture of burned gases and unburned fuel and oxidizer droplets with different incoming velocities were developed which employed the following main assumptions (Fig. 22):

1. An adiabatic and frictionless wall.
2. A one-dimensional C-J two-phase detonation propagating at constant velocity.
3. The mass efflux and the momentum loss are expressed as fractions of the corresponding values of the incoming gases and droplets.

An F-number analysis of the type first used by Adamson and Morrison[8] was carried out to yield the relations for the properties of a C-J detonation with mass bleed.

By including additional conditions of cyclic behavior and by linking the average pressure on the injection plate to the design equilibrium pressure[4], the above analysis was extended to cover the case of an annular chamber with a rotating two-phase detonation wave with mass bleed. The results of calculations in typical cases of a tube detonation and a rocket motor wave are shown in Fig. 23 and 24. A parametric study of the two phase wave with mass bleed, in the two cases of an annular chamber and the laboratory tube conditions, indicates the ways of correlating the experimental results in the laboratory to engine conditions without actually resorting to motor testing. Numerical results indicate that in order to obtain any appreciable velocity reduction for the wave the gas bleed fraction has to be large.

Estimates of the mass efflux behind the leading shock of the detonation were made using different wall porosity values. Drop breakup dynamics were included in the estimation of reaction zone length. Thus, by combining these estimates with the parametric calculations of effect of bleed, the steady state velocity of the wave with bleed can be determined. After considering numerous calculations of the above type using typical liner open-area ratio, and drop size values, the indications are that for a

steady propagating wave in the motor case it is not possible to obtain significant reductions in propagation velocity of the wave. This is mainly due to two factors: (i) the available reaction zone length is too small to obtain any significant mass bleed and (ii) the 'effective open-area' ratio of the liner is small. The situation is somewhat better in the case of typical laboratory test conditions compared to that in the engine chamber.

After reaching the above conclusions the next step taken was to study the effect of gas mass bleed on the blast waves originating from the drop combustion zone and moving towards the leading shock front. If these blast waves are sufficiently weakened by the gas bleed before they catch up with the leading shock, the sustaining mechanism for the wave propagation is disturbed, thereby causing the leading shock to slow down. A one-dimensional time-dependent finite difference technique was used with drop size, leading shock strength and wall porosity as parameters. Early results indicate that for a well developed detonation the blast wave strength is not appreciably reduced in the time it moves through the reaction zone. Correlations between the engine chamber and laboratory test conditions are to be established.

Based on the analytical work done to date, conditions for the laboratory tests on the effects of bleed on two-phase detonations, corresponding to chamber wave parameters when the liner effectiveness is optimum, will be chosen and the attenuation effectiveness of the acoustic liner will be experimentally observed.

Phase D - Film Detonations

During the past year Dr. C. S. R. Rao completed the thesis "Theoretical and Experimental Study of Film Detonations" and was awarded the Ph. D. Degree. Key parts of this thesis appear in the paper "A Two Dimensional Theory for Two Phase Detonation of Liquid Films," by C. S. R. Rao, M. Sichel, and J. A. Nicholls which was prepared for publication and appears in Combustion Science and Technology, Vol. 4, pp 209-220, 1972. In this paper and Dr. Rao's thesis the simple one dimensional film detonation theory, which is reported in "A Simple Theory for the Propagation of Film Detonations," by M. Sichel, C. S. R. Rao, and J. A. Nicholls, Thirteenth Symposium (International) On Combustion, pp 1141-1149, (1970), has been extended to take into account the effect of boundary displacement on the flow in the reaction zone.

The analysis is based on the model shown in Fig. 25 below, which shows the reaction zone of a typical film detonation from coordinates moving with the wave. In these coordinates the shock is stationary and the wall or surface of the shock tube moves with the propagation velocity U_s. A turbulent boundary layer forms immediately behind the leading shock and results in drag forces and heat transfer from the core of the reaction zone to the liquid film causing the liquid to vaporize. A key hypothesis in the analysis is that vaporization sets the rate at which the fuel in the film reacts with the oxidizer

in the core of the reaction zone. Support for this hypothesis comes from the agreement between theory and experiment as indicated below. The main difference between the one dimensional and two dimensional theories is that in the latter the displacement effect of the boundary layer upon the core flow is taken into account.

The propagation characteristics of the film detonations are obtained from the mass, momentum and energy conservation equations across the detonation front with the effects of drag, heat transfer, and boundary layer displacement within the reaction zone included in the formulation. The end of the reaction zone on the Chapman Jouquet (C-J) plane is taken as the point at which the film is completely vaporized. A detailed analysis of the Chapman-Jouguet condition shows that this choice for the C-J plane is valid as long as the fuel air ratio is not much larger than the stoichiometric value. Combustion is assumed to occur within a diffusion flame sheet imbedded in the boundary layer. The boundary layer parameters are determined by combining the results of shock tube boundary layer theory with relations which have been developed in the analysis of combustion in hybrid (liquid-solid fueled) rockets.

Theoretically computed propagation speeds, reaction zone lengths, and pressure ratios are compared to experimentally measured values in Figures 26, 27, 28 which summarize the key results of this investigation. The theory and measurements shown in

Figures 26, 27, 28 are for film detonations propagating down a square tube with internal dimensions of 1. 64 in. x 1. 64 in. filled with oxygen at atmospheric pressure and temperature and with diethylcyclohexane as the fuel. Film detonation with one, two and four walls of the shock tube wetted with fuel were considered. In these figures L is the reaction zone lengths, p_3/p_1 is the pressure ratio across the detonation and u_s/u_{so} is the ratio of the actual propagation velocity u_s to the propagation velocity u_{so} of a premixed gaseous detonation without losses and with the same fuel and oxidizer. Results from both the one and two dimensional theories are shown.

Figures 26, 27, 28 indicate good agreement between the analysis and experimental measurements and support the model of the film detonation described above. In particular it appears that vaporization is the rate limiting process, at least in the case considered here with very thin films and overall fuel air ratios of the order of the stoichiometric value.

The effect of diluting the oxygen with nitrogen has also been investigated. Theory and experiment are compared in Figures 29, 30, 31 for oxygen mass fractions of 1. 0, . 89, and 0. 675. Again agreement between theory and experiment was good. In the experiments it was found that film detonations would not propagate when the dilution exceeded a certain critical value. Thus it was im-

possible to detonate diethylcyclohexane films in air. The conclusions may, of course, change for different fuels, particularly fuels with a high vapor pressure. Also, higher initiation energies may lead to steady detonation in air.

At the present time a contractor report describing the details of the film detonation analysis is under preparation. The study of film detonation will then be terminated.

Phase E - Theoretical Analysis of a Tangential Two-Phase Detonation

This phase of the research has been devoted to a theoretical treatment of a tangential mode strong discontinuity type of instability. The major portion of the work was completed and written up in the past year. A detailed treatment of the work appears as the Ph. D. thesis of I-wu Shen, 1971, entitled, "Theoretical Analysis of a Rotating Two-Phase Detonation in a Liquid Propellant Rocket Motor." A paper, based on this work with the same title, was presented at the Third International Colloquium on Gas Dynamics of Explosions and Reactive Systems, University of Marseille, Marseille, France, September, 1971. This paper will appear soon in Astronautica Acta. A short summary of the work completed and that in progress will now be given.

The analysis assumes that a one-dimensional two-phase detonation propagates at some constant, but unknown, angular velocity in a thin annular combustion chamber. Thus, no radial variations are taken into account. The walls are taken to be adiabatic and frictionless. It is assumed that the drops remain at their initial condition until they are converted to gases in the thin reaction zone. The detonation is treated as a discontinuity and the flow between waves is assumed isentropic with no interaction between drops and the burned gases. Further, the influence of the wave on propellent injection rate and combustion efficiency is neglected. The rotating wave is

assumed to decay to a sound wave as the nozzle is approached.

In this problem, as posed, there are 9 variables inasmuch as the wave velocity is unknown a priori. The variables in addition to wave velocity are the pressure, density, temperature and gas velocity immediately upstream as well as immediately downstream of the wave. In order to determine these 9 unknown, 9 equations are needed. These are obtained by employing the jump conditions for a two-phase mixture of burned gases, unburned fuel and oxidizer droplets. The cyclic condition provides additional information and, finally, the pressure distribution along the injector plate (determined by the method of characteristics) is integrated numerically to obtain the average pressure which is then linked to the design equilibrium chamber pressure. The analysis then predicts the variation of wave strength (as measured by pressure ratio or wave velocity and assuming the wave exists) with nozzle area ratio, specific heat ratio, injection velocity, impingement distance, equilibrium chamber sound speed, chamber diameter, and fuel distribution.

It is found that the pressure ratio across the wave may be reduced (i. e. stabilizing) by reducing the contraction ratio, reducing the propellant flux density at the outer periphery near the injection plate. increasing the injection velocity, reducing the chamber diameter, and decreasing the chamber speed of sound. The wave strength is independent of chamber length and propellant mass flow. An increase in the

latter increases the pressure level of the engine but the pressure ratio across the wave remains the same.

A further portion of the analysis has considered the influence of drop size insofar as it affects the validity of the analysis, and hence the possibility of realizing such an instability.

A comparison of the predicted results with the few available experimental results are very encouraging, both as to the pressure predictions and limits of validity of the analysis.[9]

A NASA report streamlining the above analysis for the designer's purpose is being prepared. Also, a small effort is continuing to include the first effects of radial variations such as would exist in a cylindrical chamber. The equations have been set-up for this addition but predicted results are not yet available.

REFERENCES

1. Kauffman, C.W. and Nicholls, J.A., "Shock Wave Ignition of Liquid Fuel Drops," AIAA 8th Aerospace Sciences Meeting, New York, NY (1970).

2. Kauffman, C.W., Nicholls, J.A., and Olzmann, K.A., "The Interaction of an Incident Shock Wave with Liquid Fuel Drops," AIAA 9th Aerospace Sciences Meeting, New York, NY (1971).

3. Kauffman, C.W., "Shock Wave Ignition of Liquid Fuel Drops," Ph.D. Thesis, The University of Michigan, 1971.

4. Nicholls, J.A., "Two Phase Detonation Studies Conducted in 1970," Nasa CR 72866, March 1971.

5. MacCormack, R.W., "The Effect of Viscosity in Hypervelocity Impact Cratering," AIAA Paper No. 69-354, AIAA Hypervelocity Impact Conference, May 1969.

6. Nicholls, J.A., "Two Phase Detonation as Related to Rocket Motor Combustion Instability," NASA CR 72532, Feb. 1969.

7. Nicholls, J.A., "Two Phase Detonation as Related to Rocket Motor Combustion Instability," NASA CR 72668, March 1970.

8. Adamson, T.C. and Morrison, R.B., "On the Classification of Normal Detonation Waves," Jet Propulsion, August 1955.

9. Clayton, R.M., Rogero, J.G., and Sotter, J.G., AIAA J., Vol. 6, No. 7, July 1968, pp. 1252-1259.

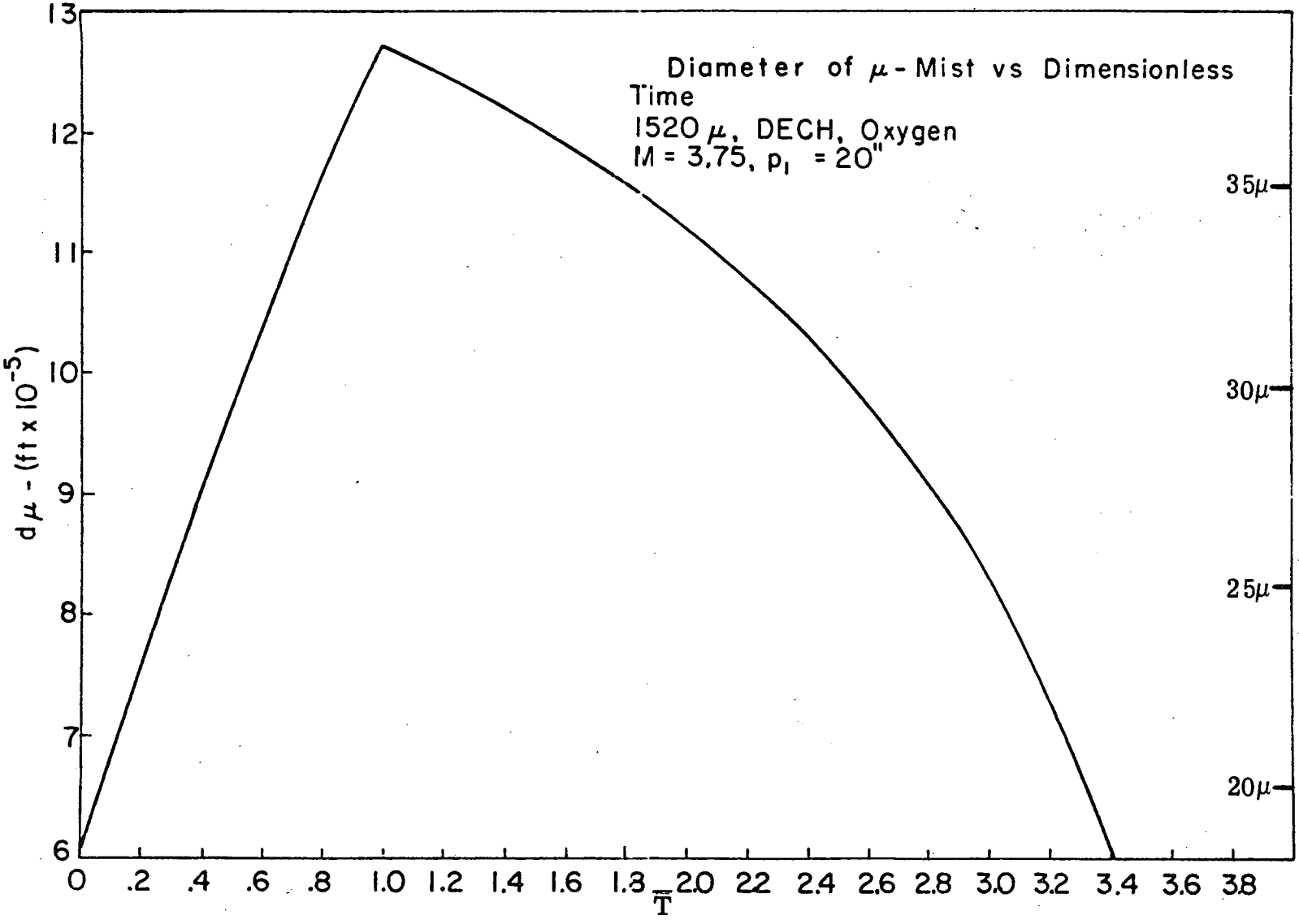

Fig. 1. Diameter of Micromist vs Dimensionless Time, 1520μ DECH Drops.

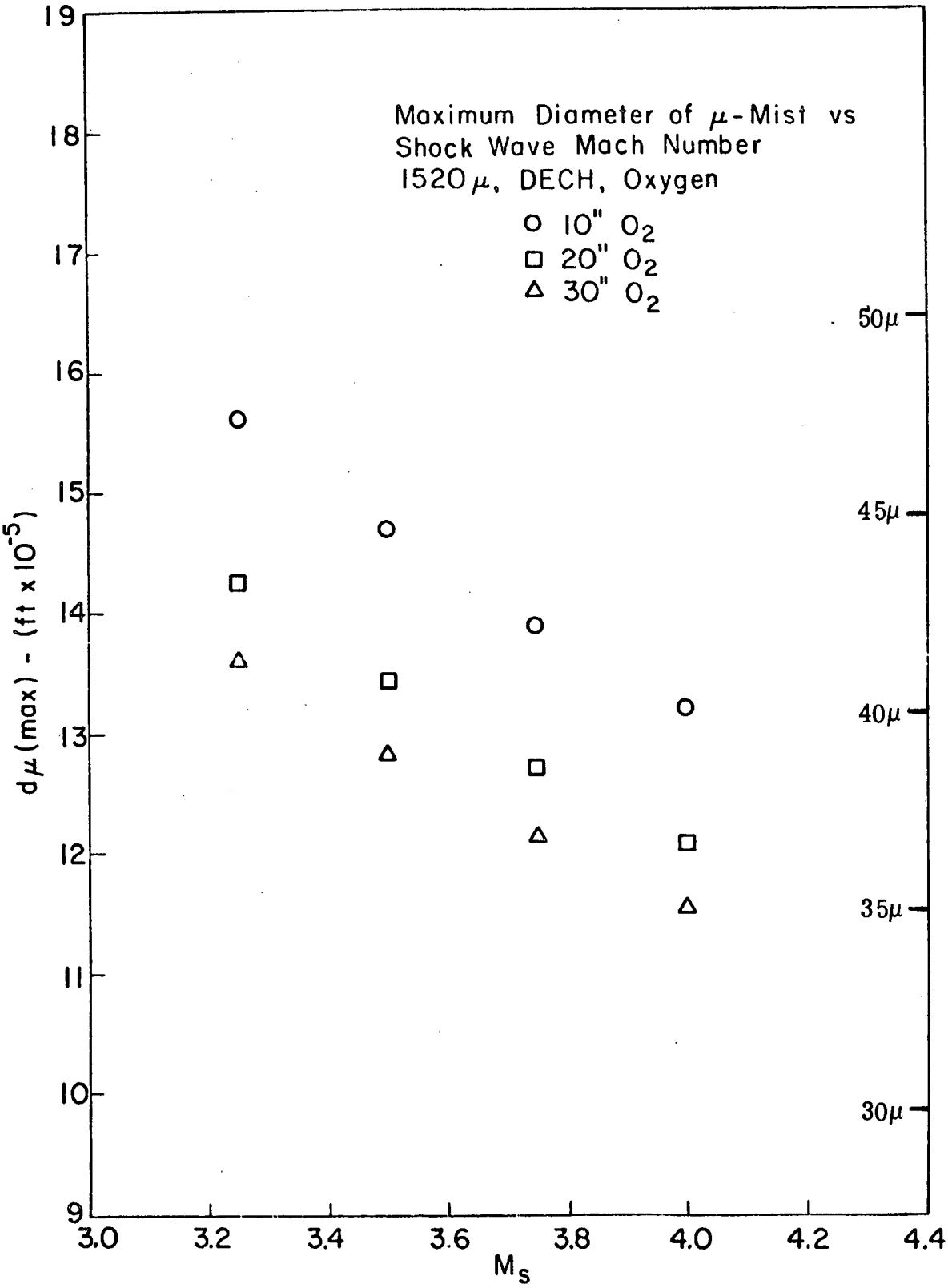

Fig. 2. Maximum Diameter of Micromist vs Shock Wave Mach Number, 1520μ DECH Drops.

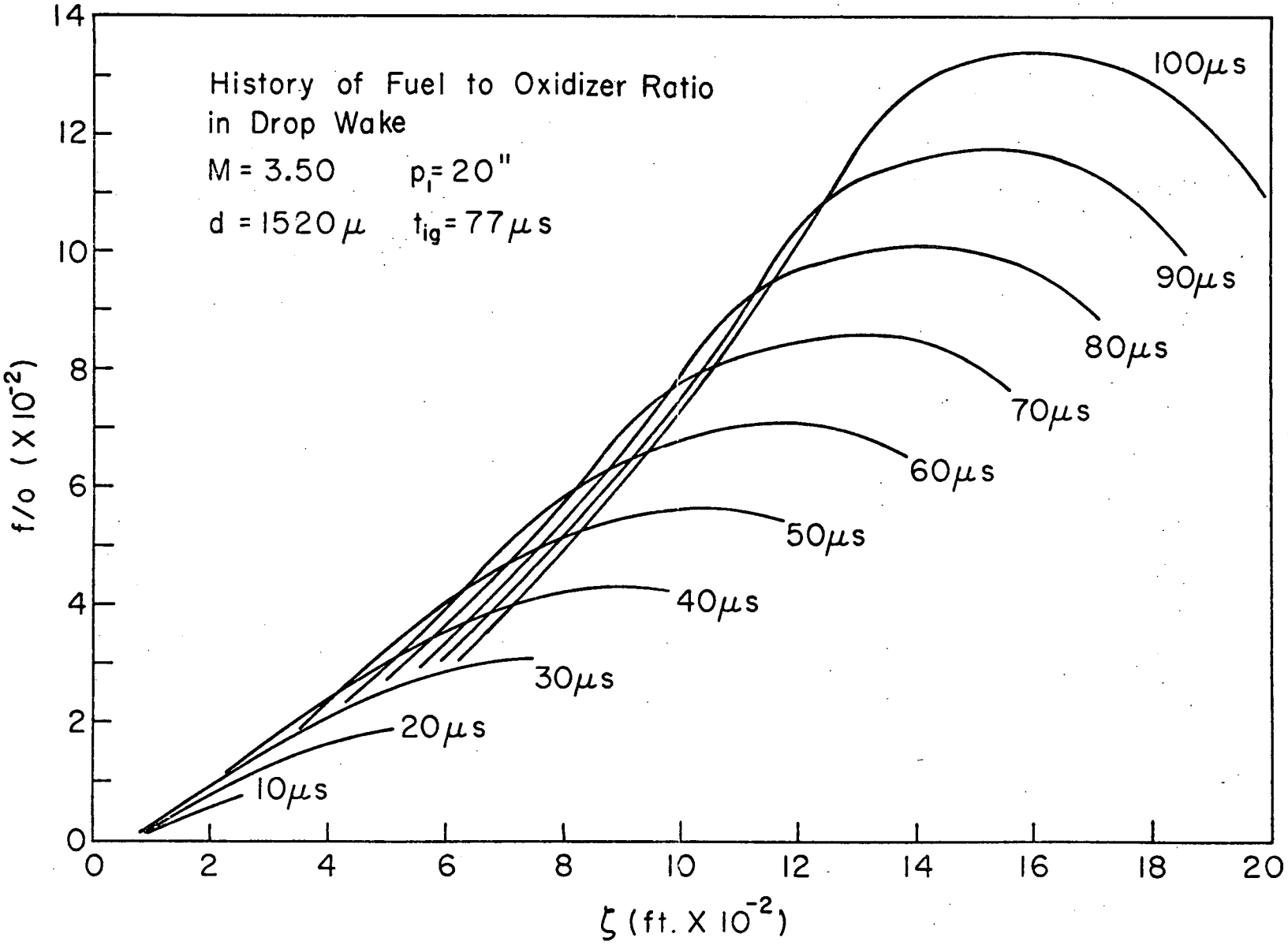

Fig. 3. Time and Location Dependence of Fuel to Oxidizer Ratio, 1520μ DECH Drops, M_s = 3.50.

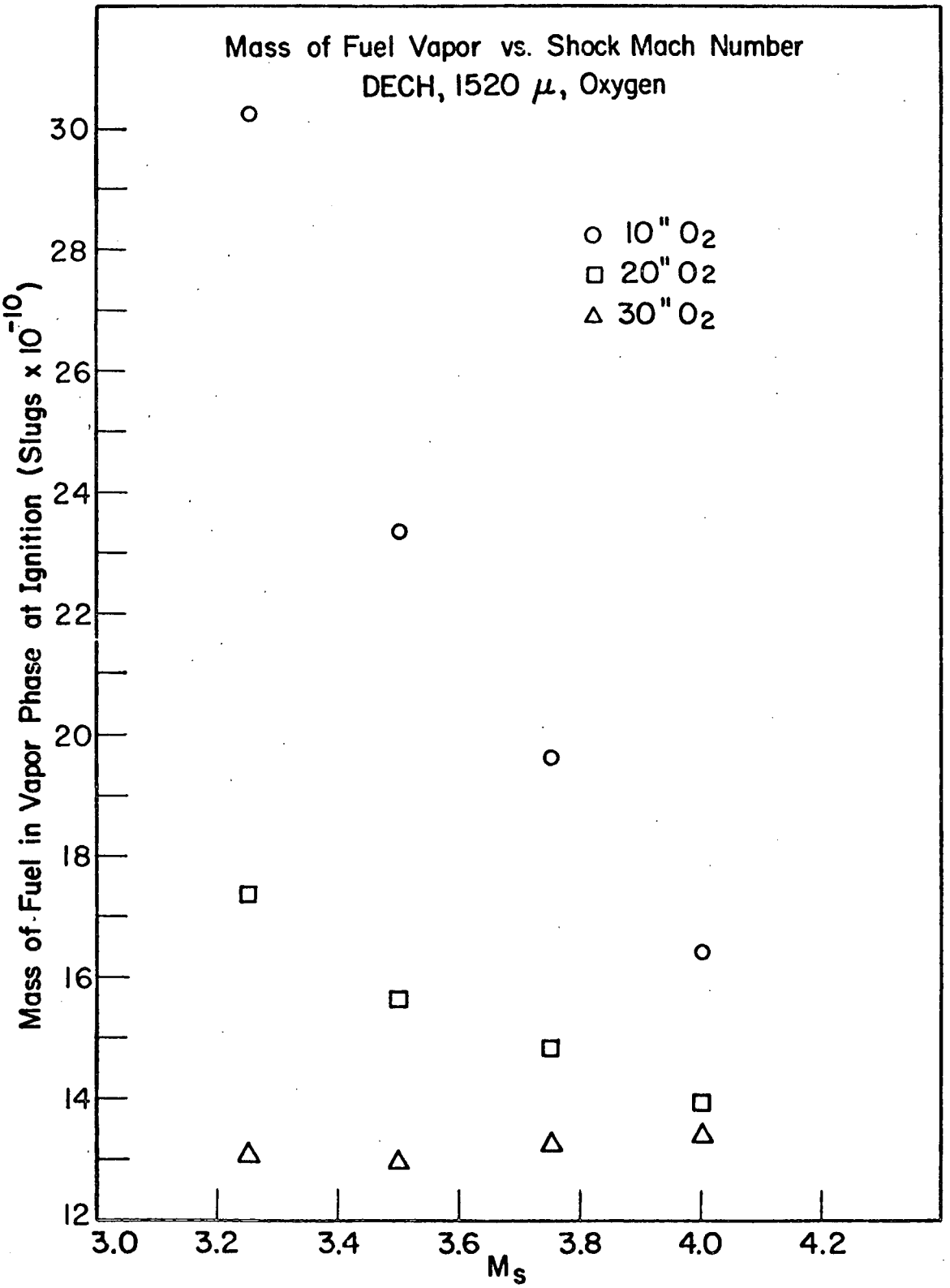

Fig. 4. Mass of Fuel Vapor vs Incident Shock Wave Mach Number, 1520μ DECH Drops.

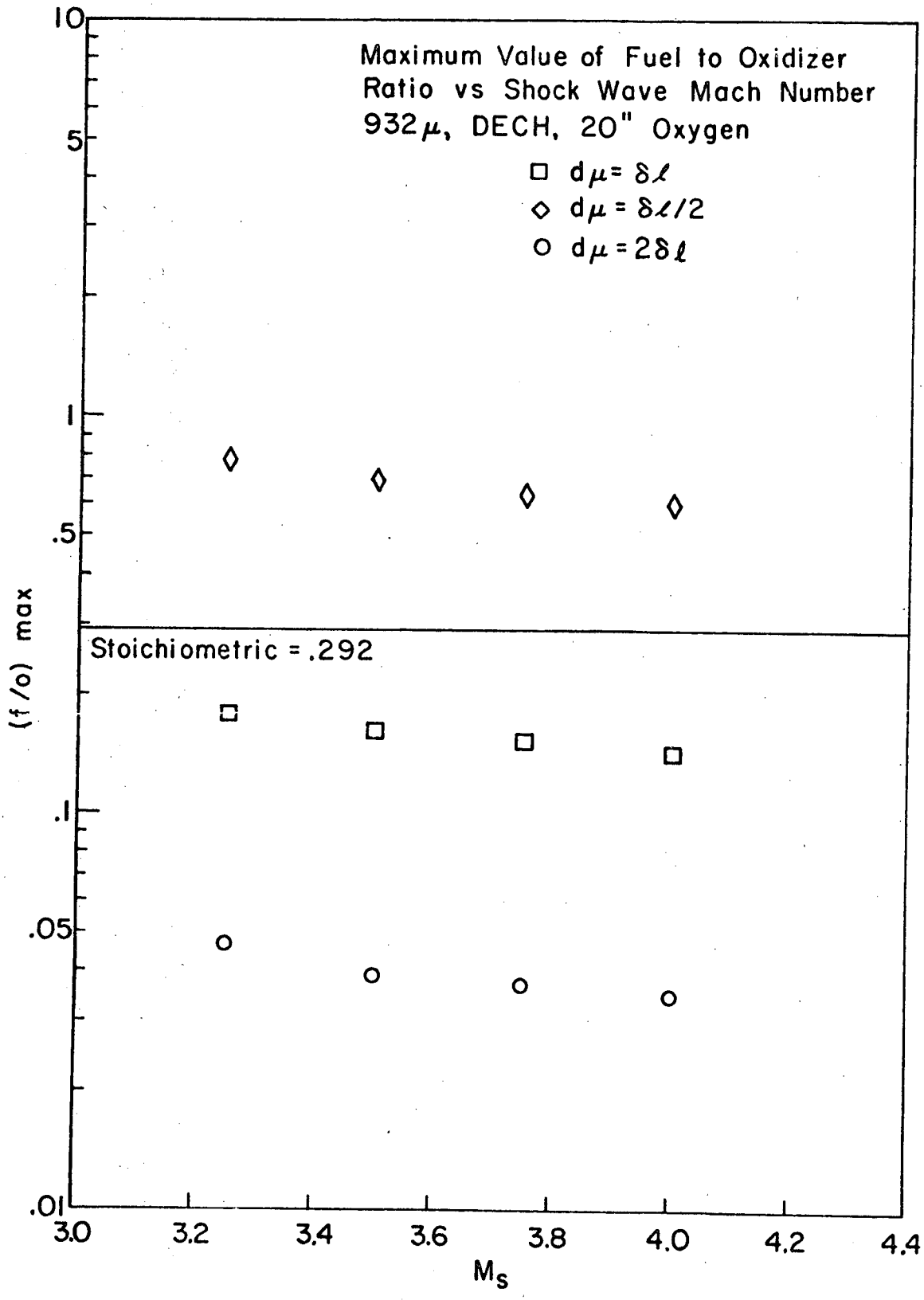

Fig. 5. Maximum Value of Fuel to Oxidizer Ratio vs Incident Shock Wave Mach Number, Various Micromist Sizes.

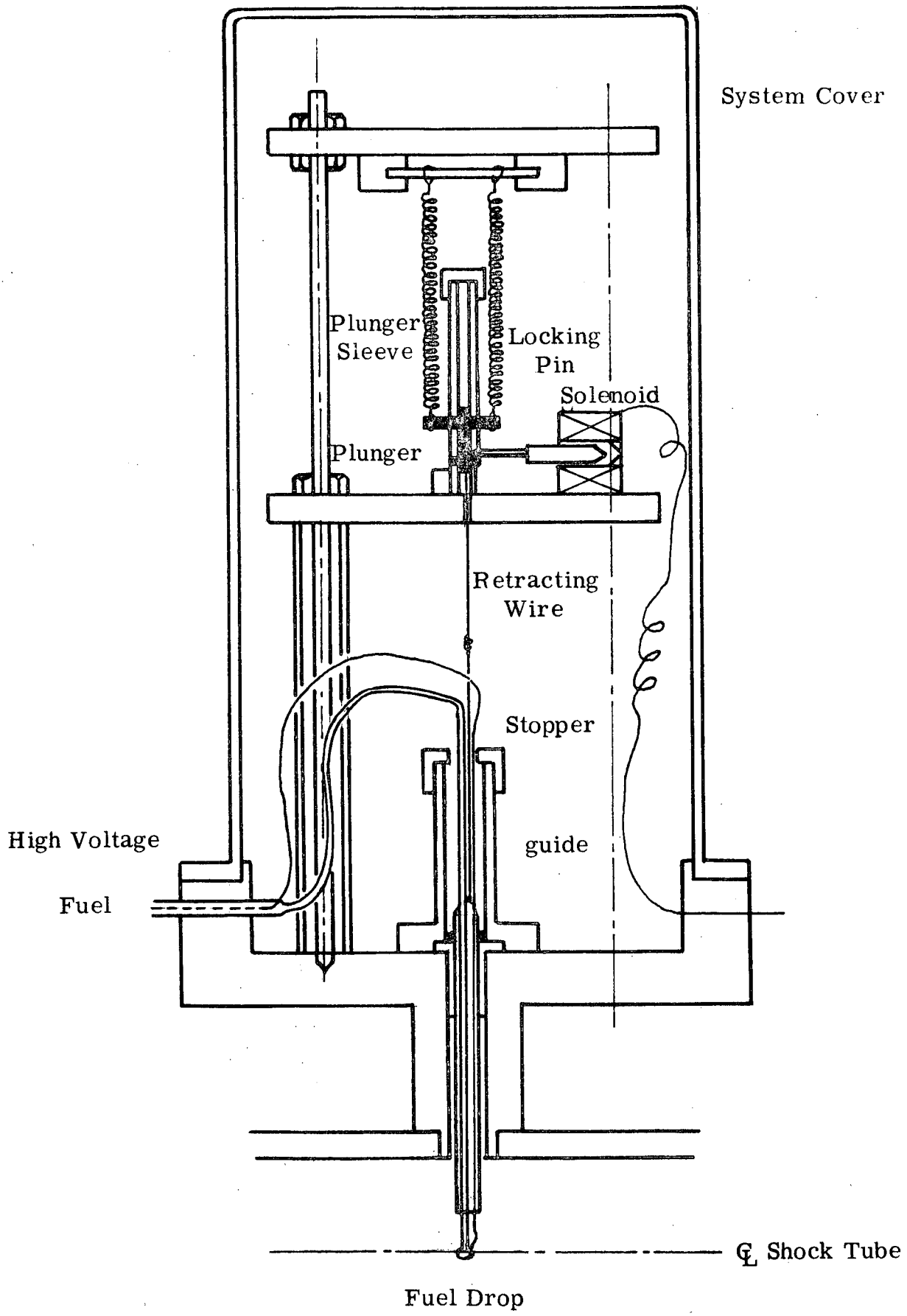

Figure 6. Ignited Drop Injection System.

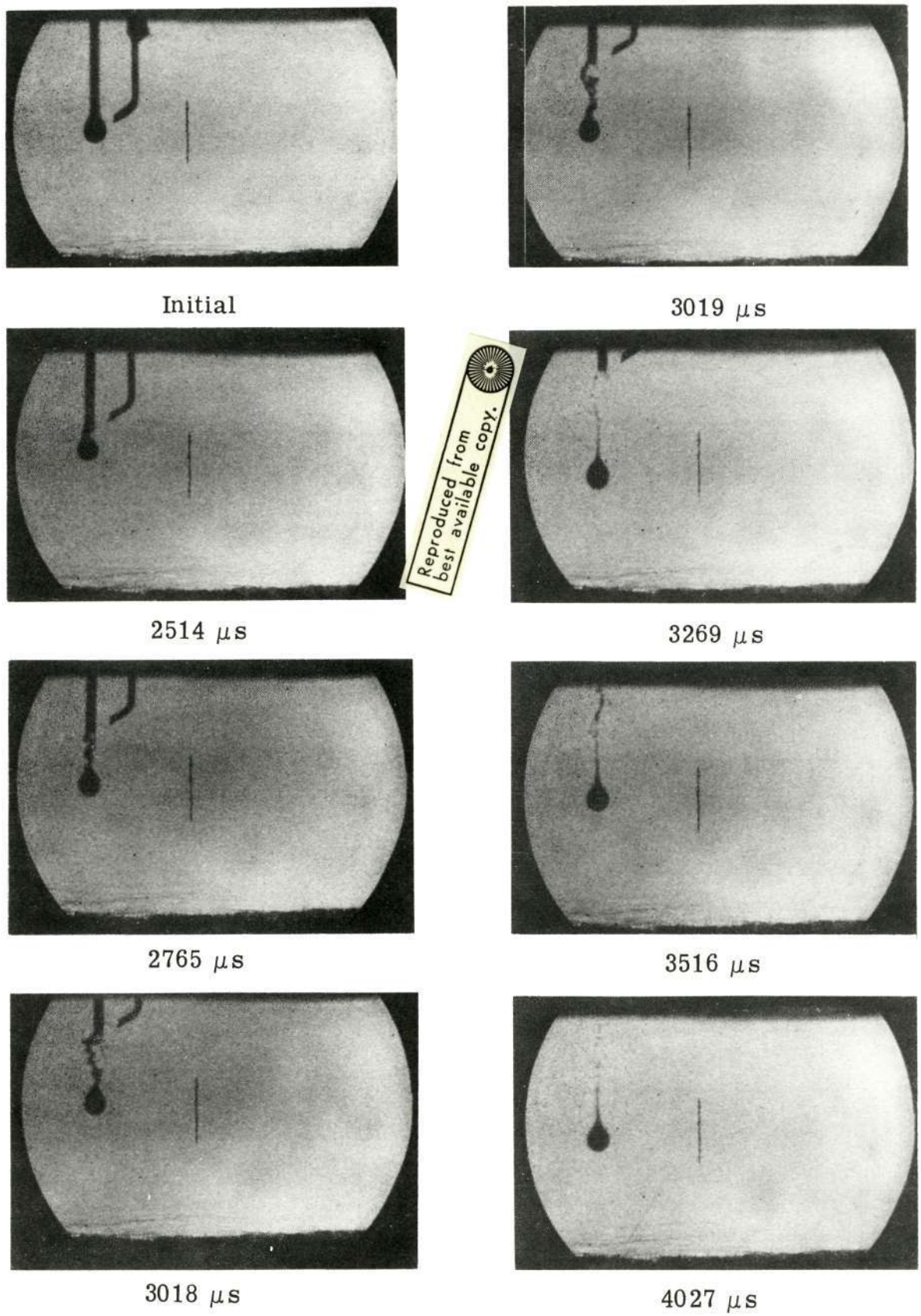

Fig. 7. Drop Formation; Non-Burning.

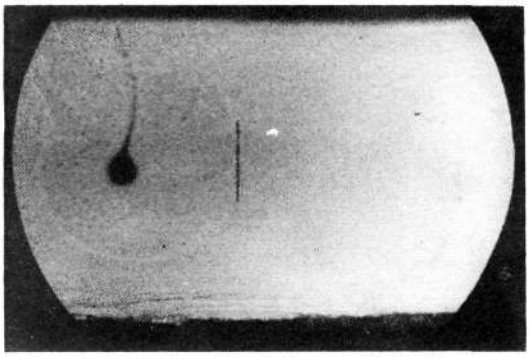

Undisturbed

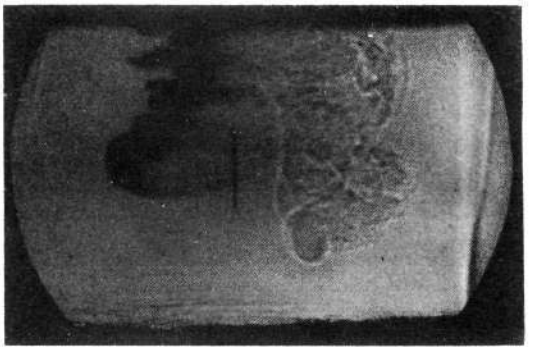

Run No. 11 50 μs

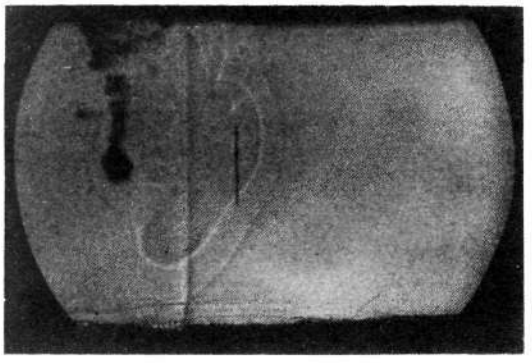

Run No. 8 10 μs

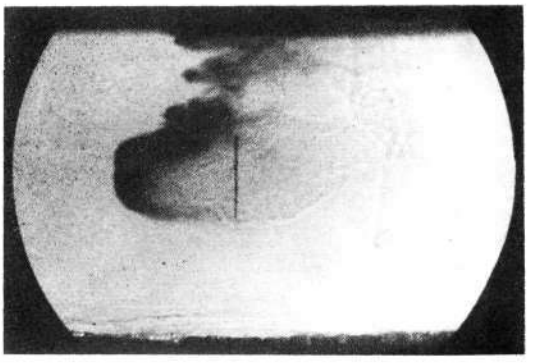

Run No. 12 72 μs

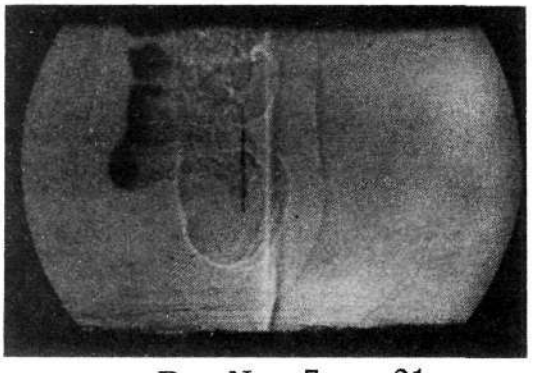

Run No. 7 21 μs

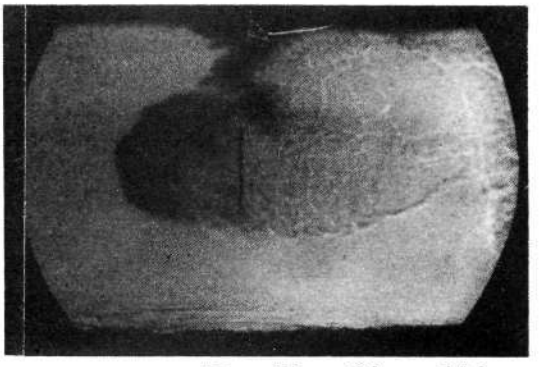

Run No. 13 100 μs

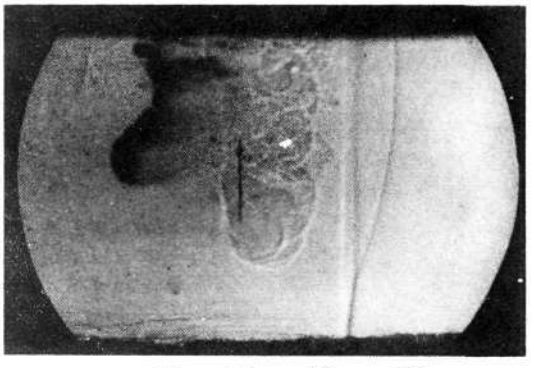

Run No. 10 32 μs

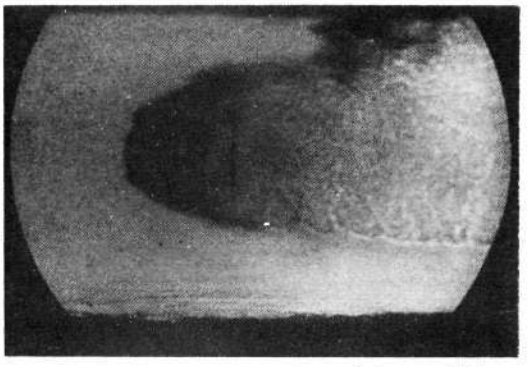

Run No. 14 149 μs

Fig. 8. Shock Wave Interaction of Burning DECH Drops. $M_s = 1.55$, $d = 2040\mu$.

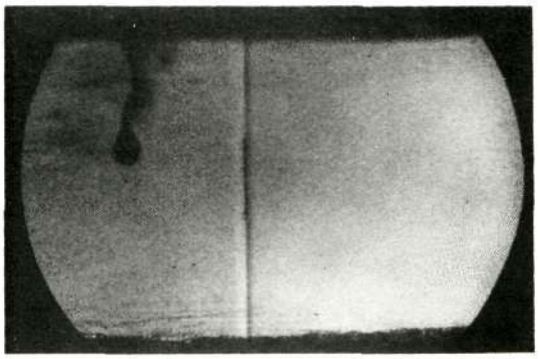

Run No. 16 17 μs

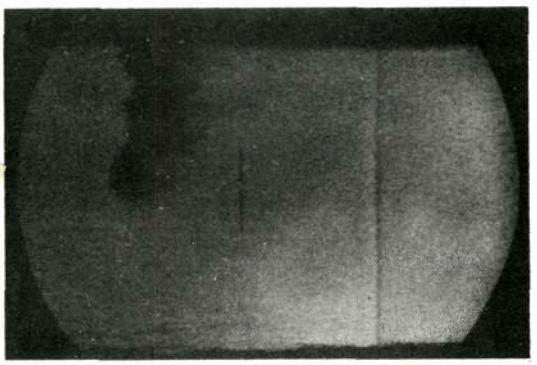

Run No. 1 31 μs

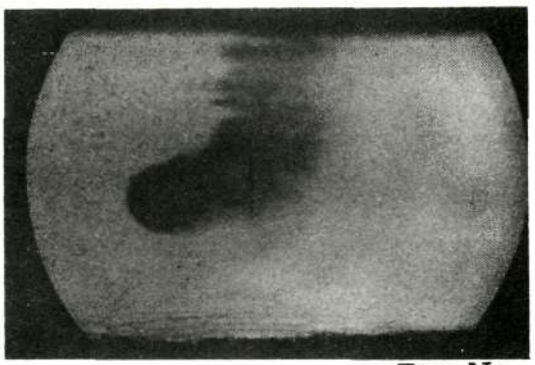

Run No. 3 63 μs

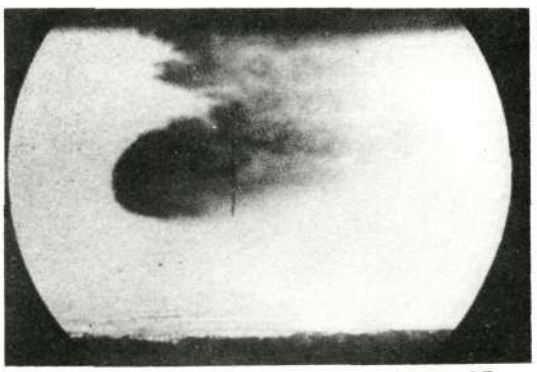

Run No. 4 93 μs

Fig. 9. Shock Wave Interaction of Non-Ignited DECH Drops. $M_s = 1.56$, $d = 2040\mu$.

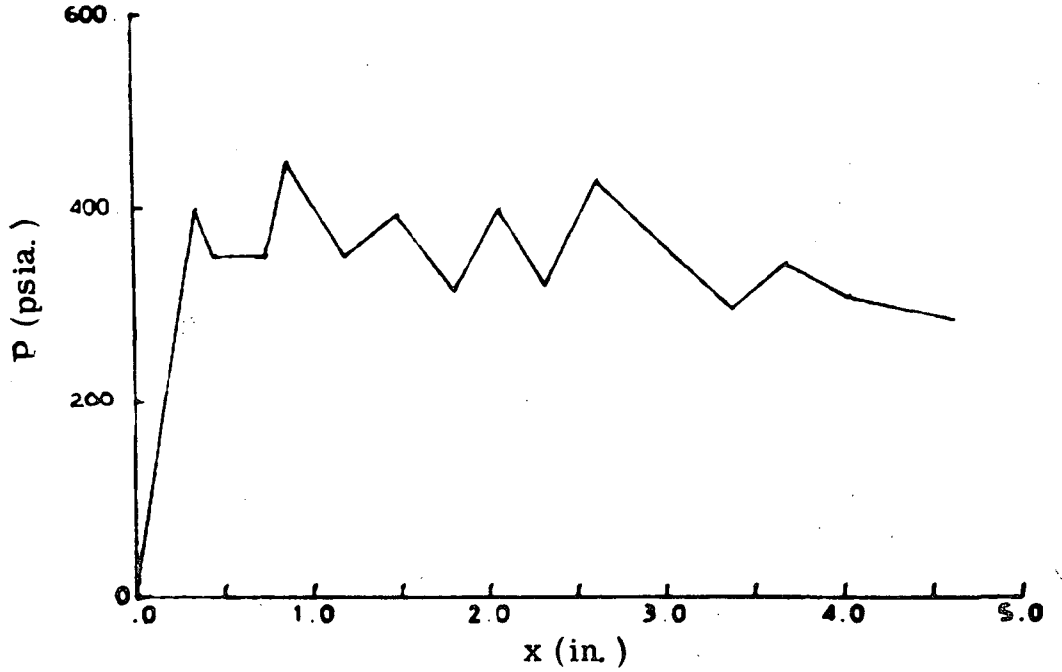

(a)

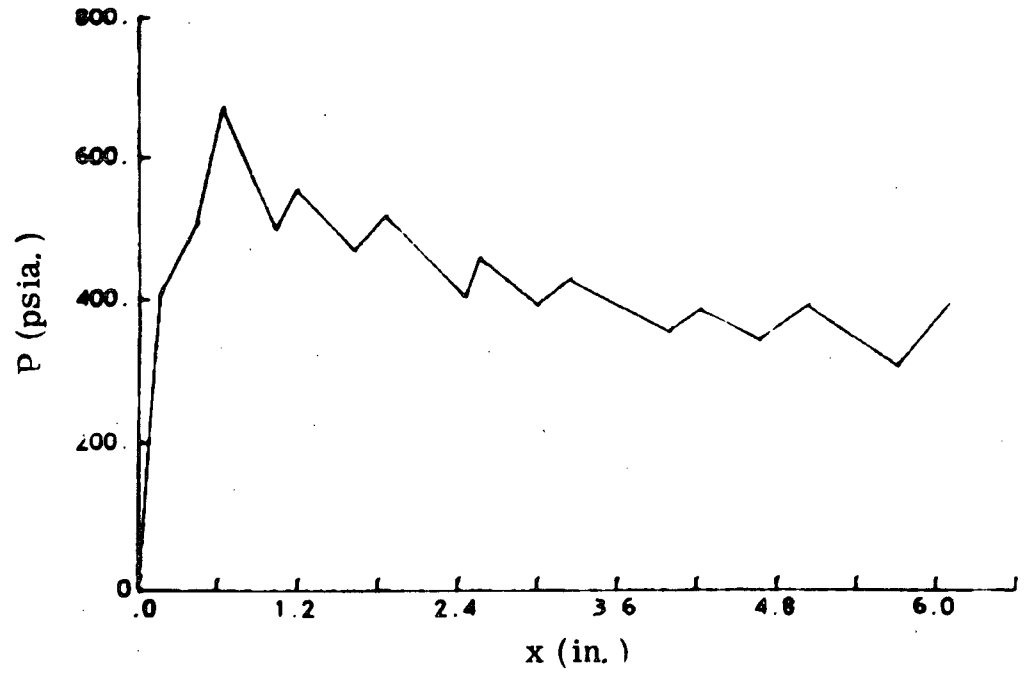

(b)

Fig. 10. Pressure Distribution behind Detonation; $\phi_T = .8$, $P_1 = 1$ atm; Upper: Monodisperse Spray, 1300μ Diameter Drops; Lower: Bimodal Spray, 300μ and 1300μ Diameter Drops, $a_{1300} = .525$.

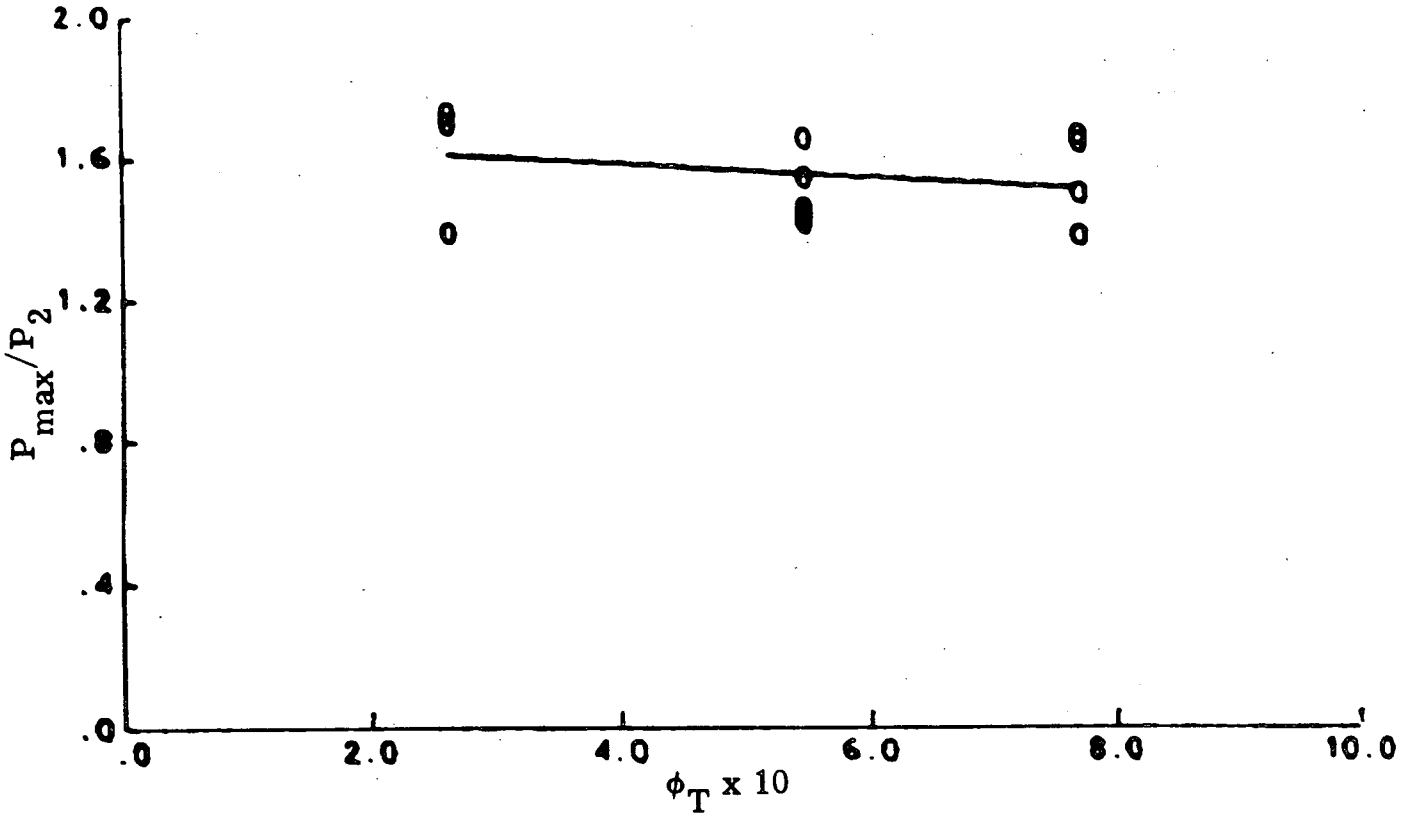

Fig. 11. Maximum Overpressure vs Equivalence-Ratio in Spray of 300μ and 750μ Diameter Drops; $a_{750} = .55$, $P_1 = 1$ atm.

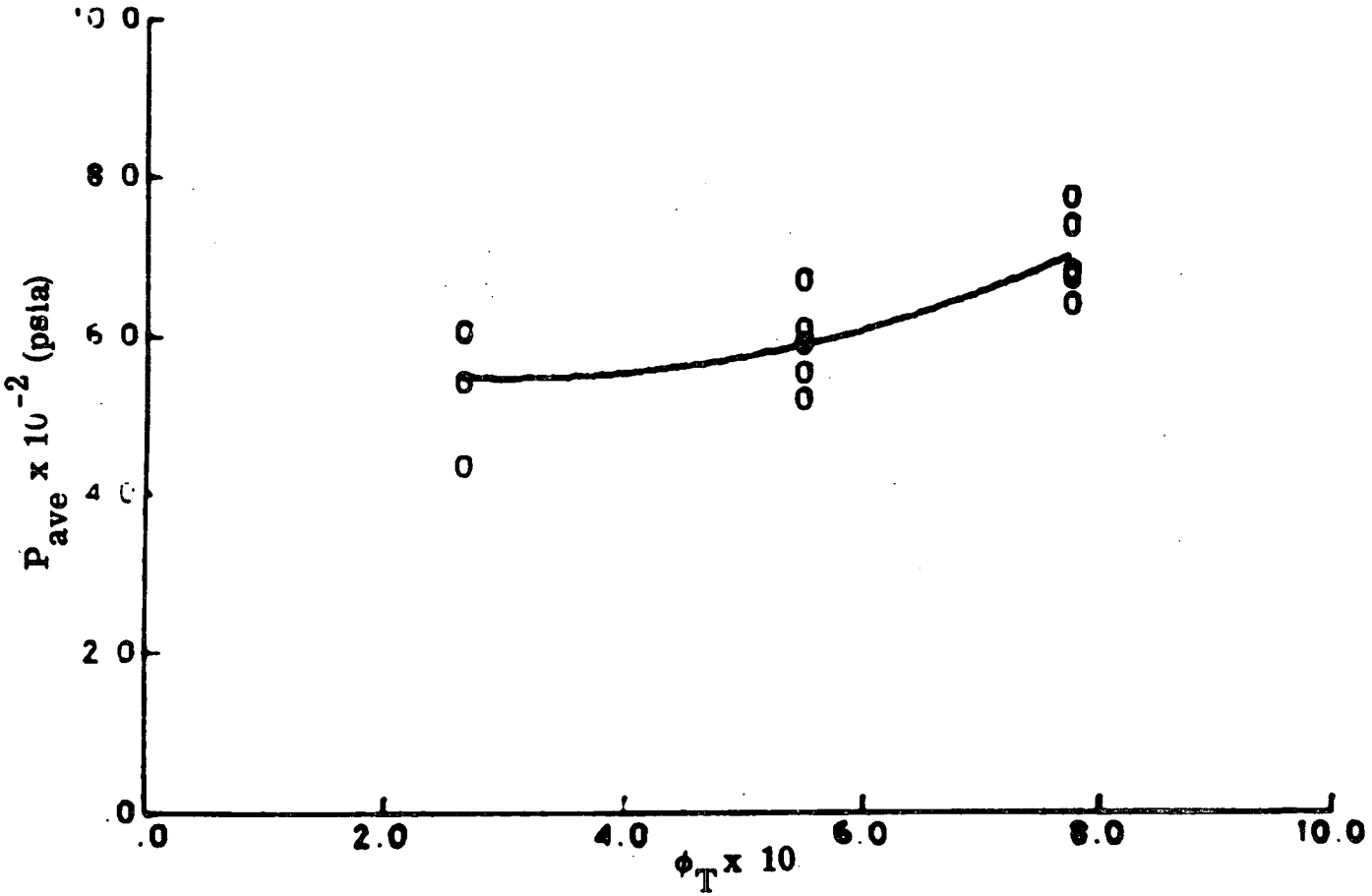

Fig. 12. Average Pressure During Initial 30 μsec Period After Passage of Leading Shock in Spray of 300μ and 750μ Diameter Drops vs Equivalence Ratio; $a_{750} = 0.55$, $P_1 = 1$ atm.

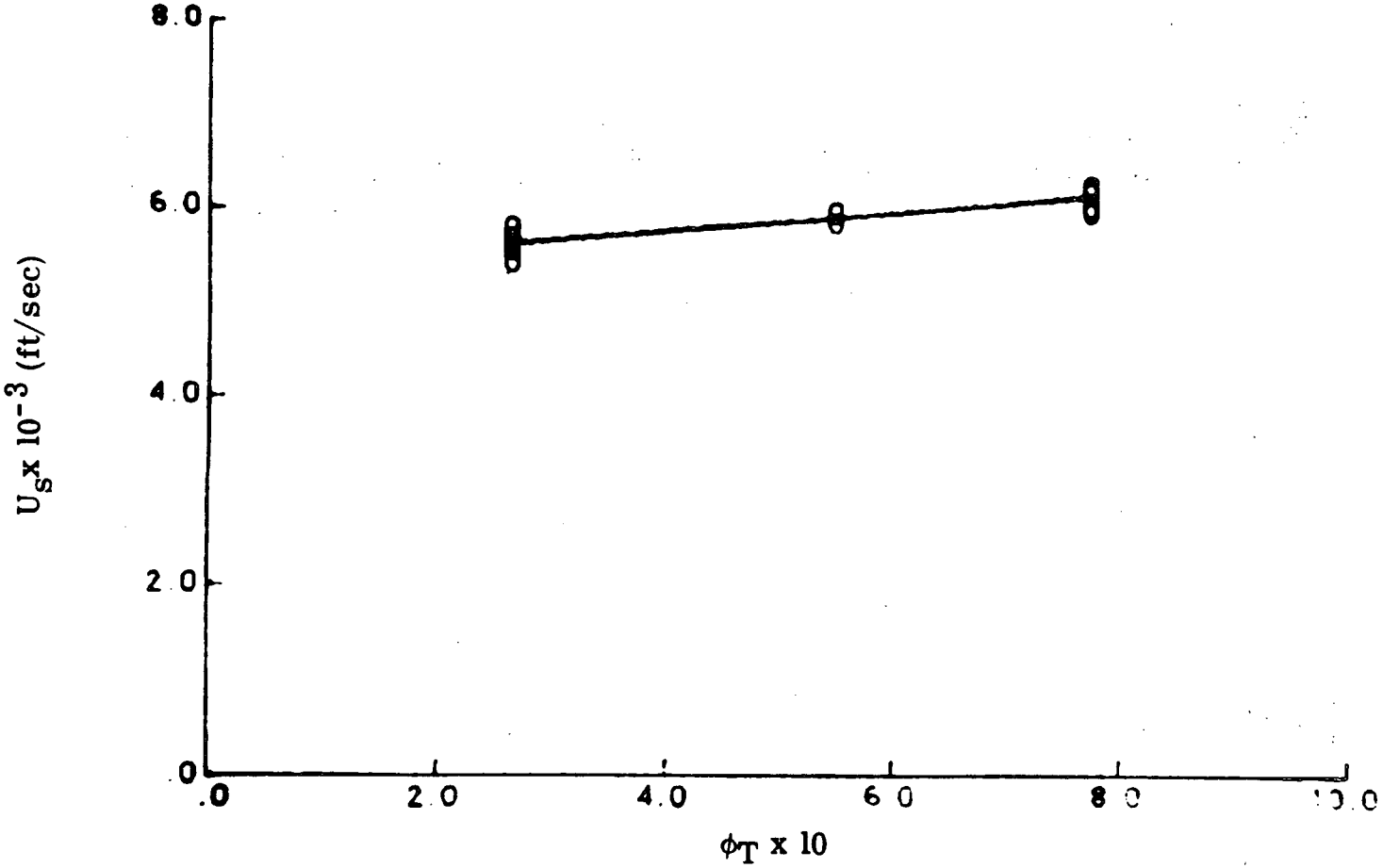

Fig. 13. Detonation Velocity vs Equivalence-Ratio in Spray of 300μ and 750μ Diameter Drops; $a_{750} = .55$.

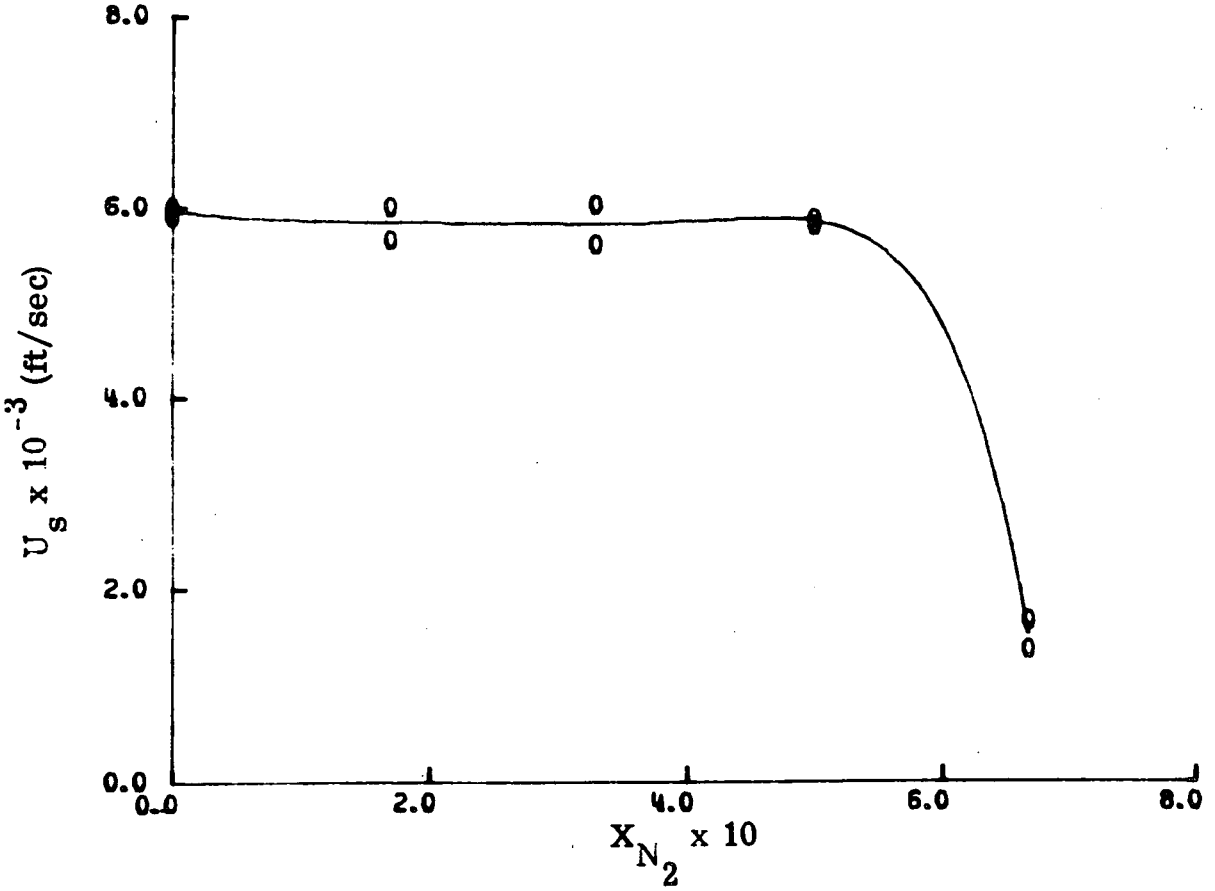

Fig. 14. Detonation Velocity vs Nitrogen Mole Fraction;
$D_o = 750\mu$, $P_1 = 1$ atm, $\phi = 0.914$.

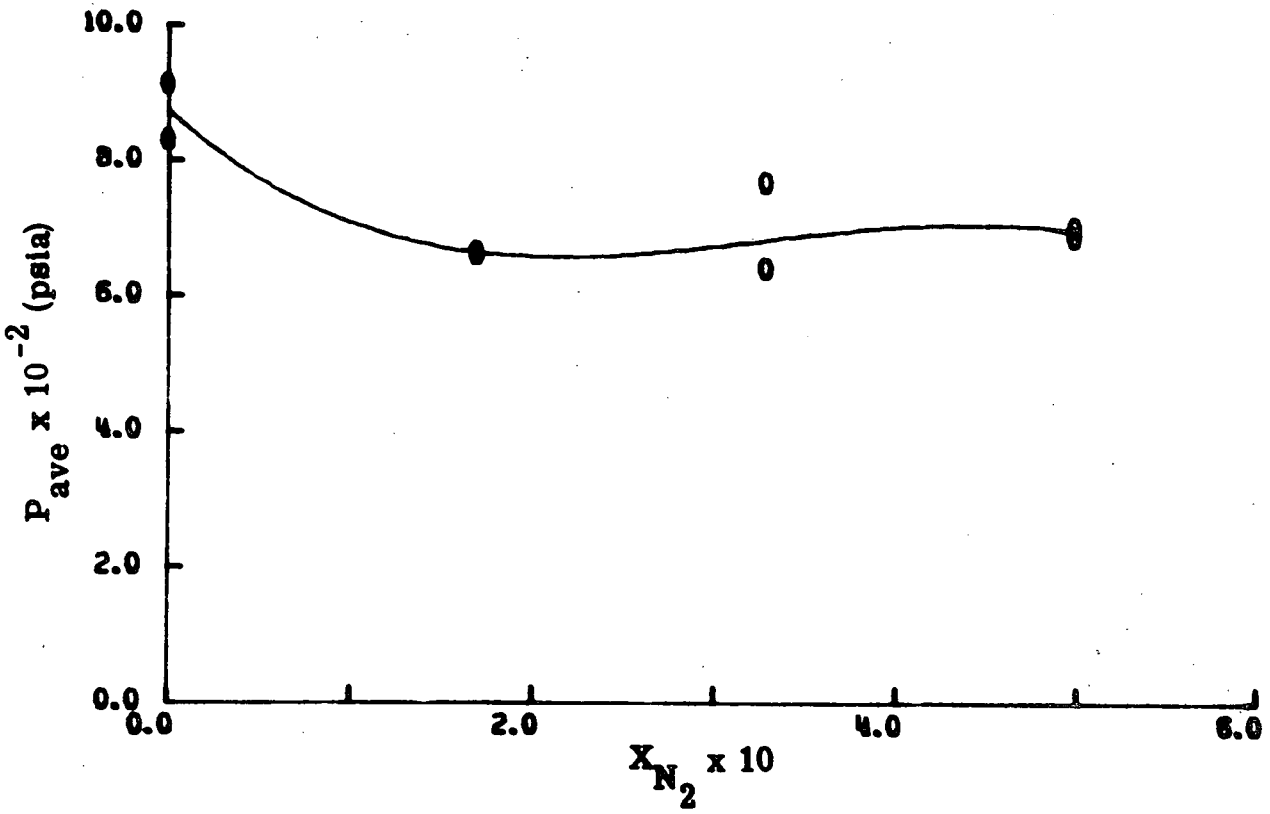

Fig. 15. Average Pressure during Initial 30 μsec Period after Passage of Leading Shock in Spray of 750μ Diameter Drops vs Nitrogen Mole Fraction; Constant Initial Charge-Gas Mixture Pressure of 1 atm; ϕ = .914.

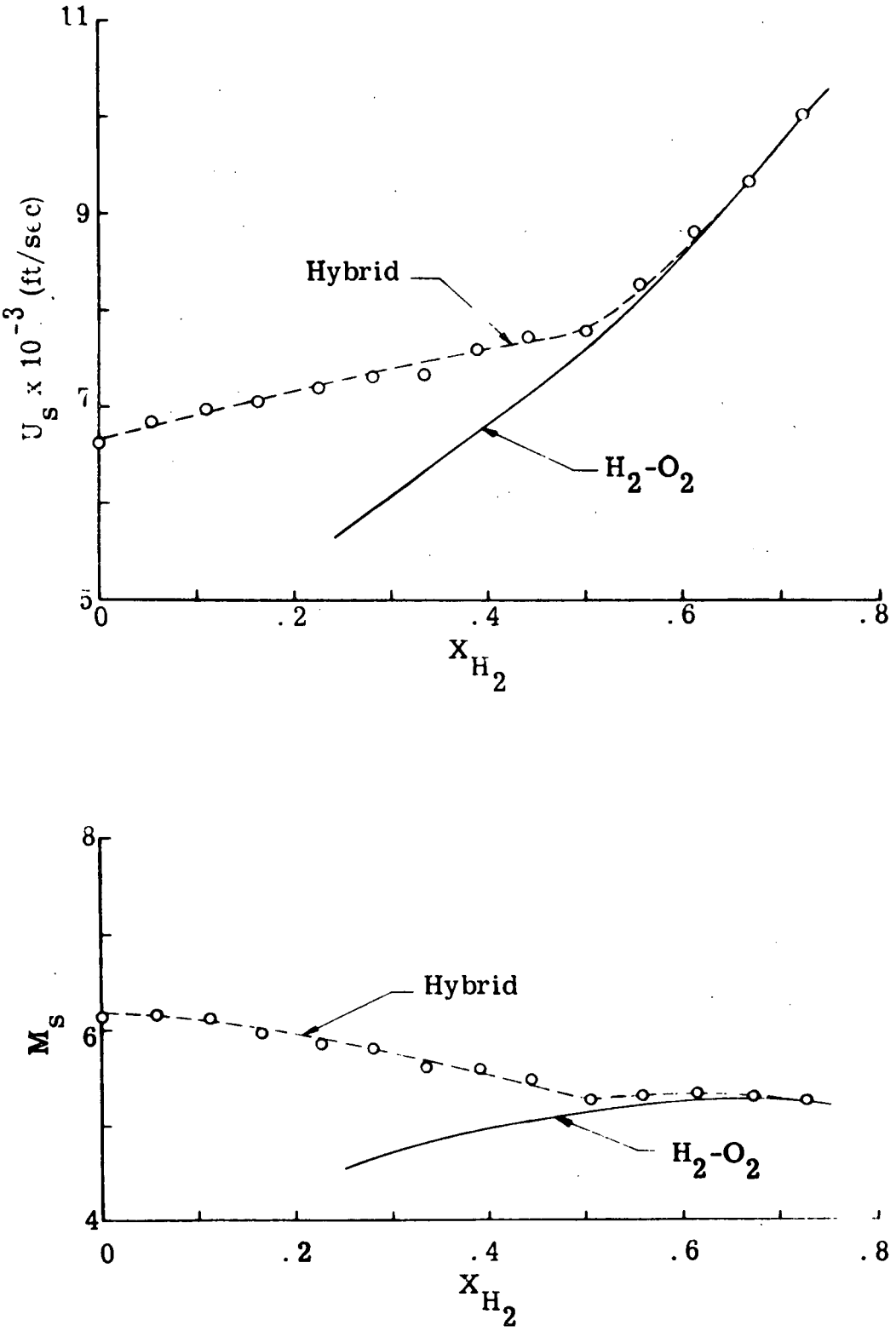

Fig. 16. Detonation Velocity and Mach Number vs Hydrogen Mole Fraction in Hybrid DECH-O_2, H_2-O_2 System; P_1 = 1 atm, ϕ_{DECH} = 1.09 (Based on Initial O_2 Concentration).

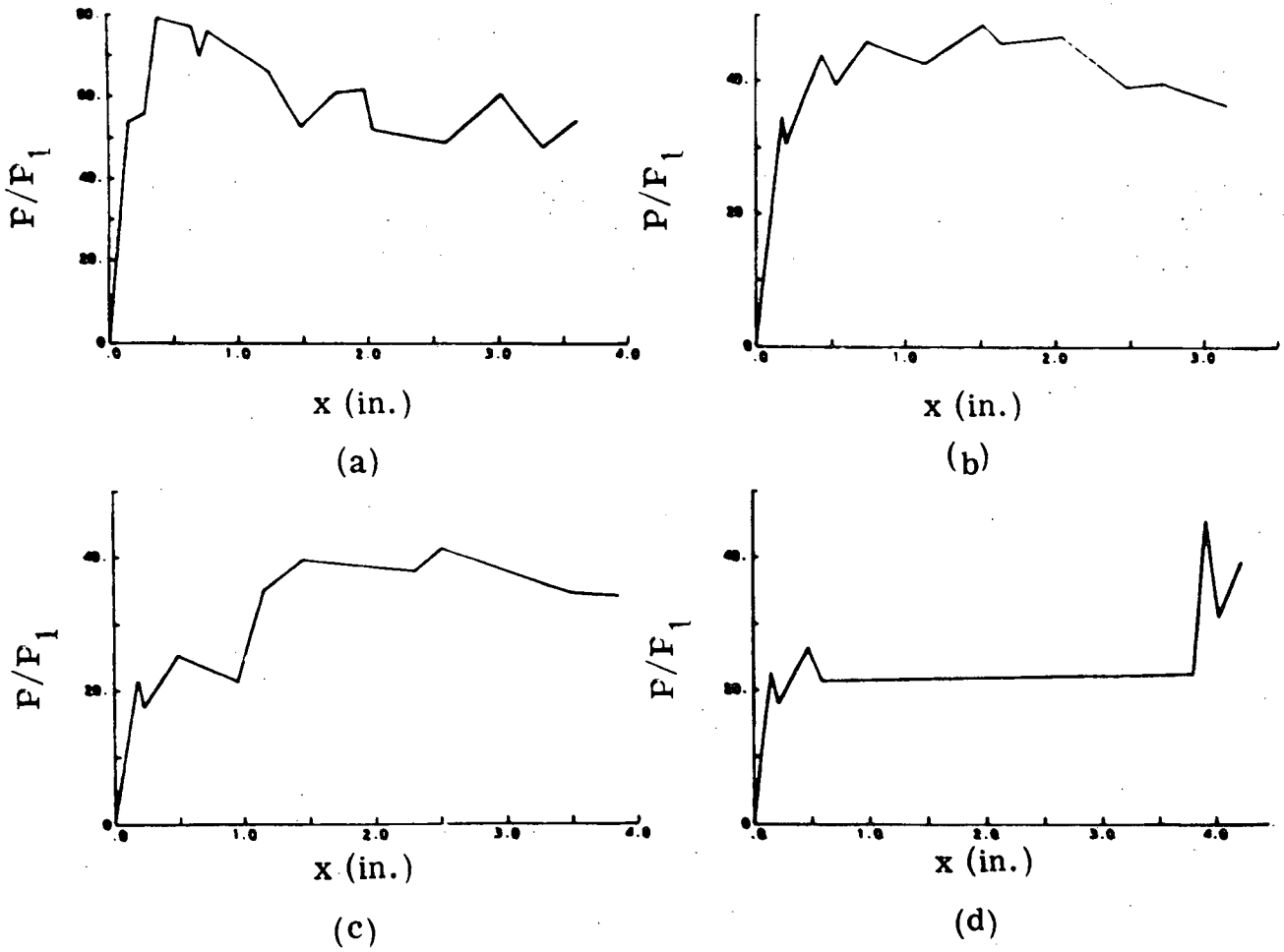

Fig. 17. Pressure Structure of Hybrid Detonation; P_1 = 1 atm, ϕ_{DECH} = 1.09 (Based on Initial O_2 Concentration); (a) ϕ_{H_2} = 0.0, X_{H_2} = 0.0; (b) ϕ_{H_2} = 0.249, X_{H_2} = 0.333; (c) ϕ_{H_2} = 0.5, X_{H_2} = 0.4; (d) ϕ_{H_2} = 0.625, X_{H_2} = 0.555.

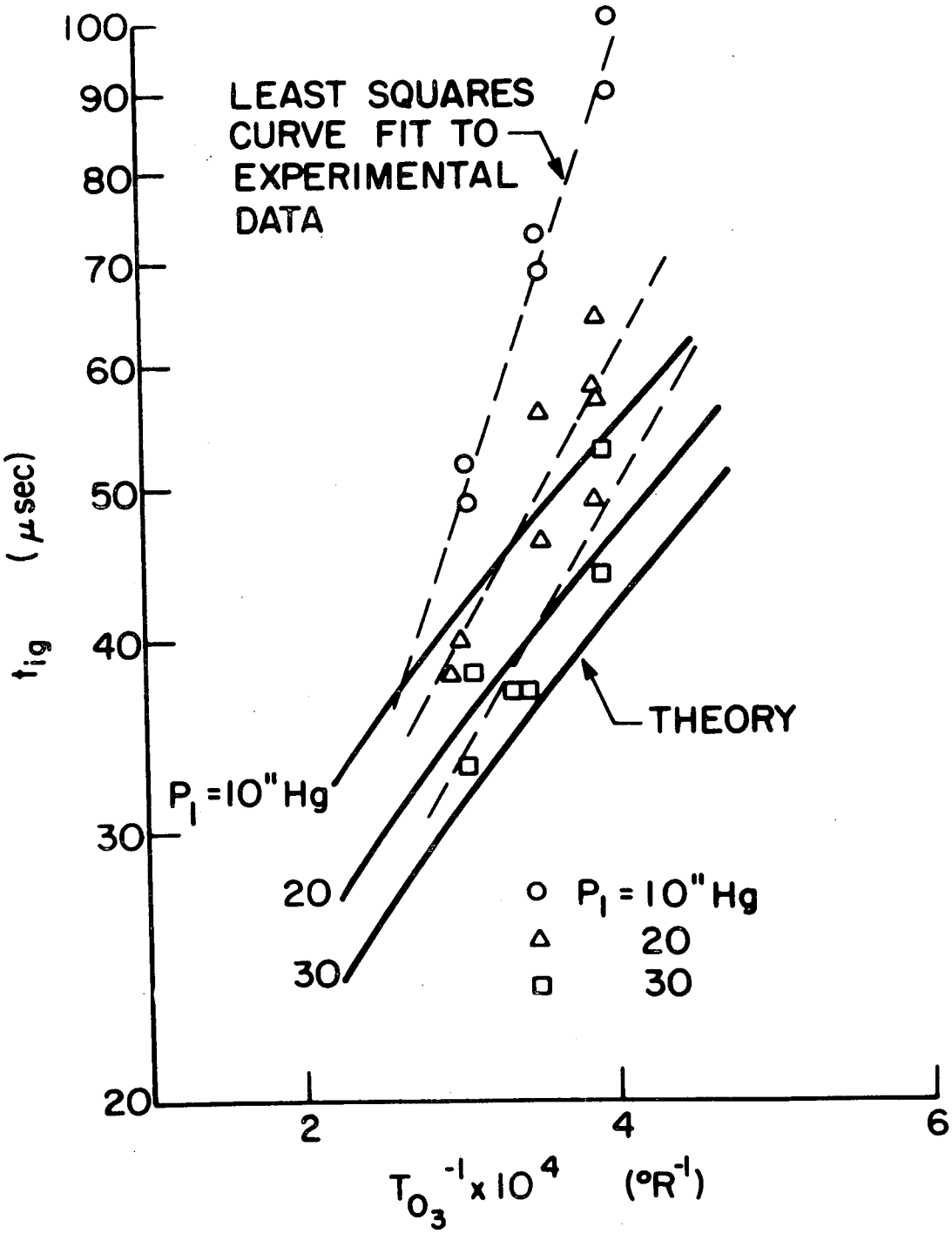

Fig. 18. Comparison of Theoretical Ignition Time with Experimental Data, Whole-Wake Thermal Theory; DECH Drops in Pure O_2, D_o = 930μ (Experimental Data from Ref. 3).

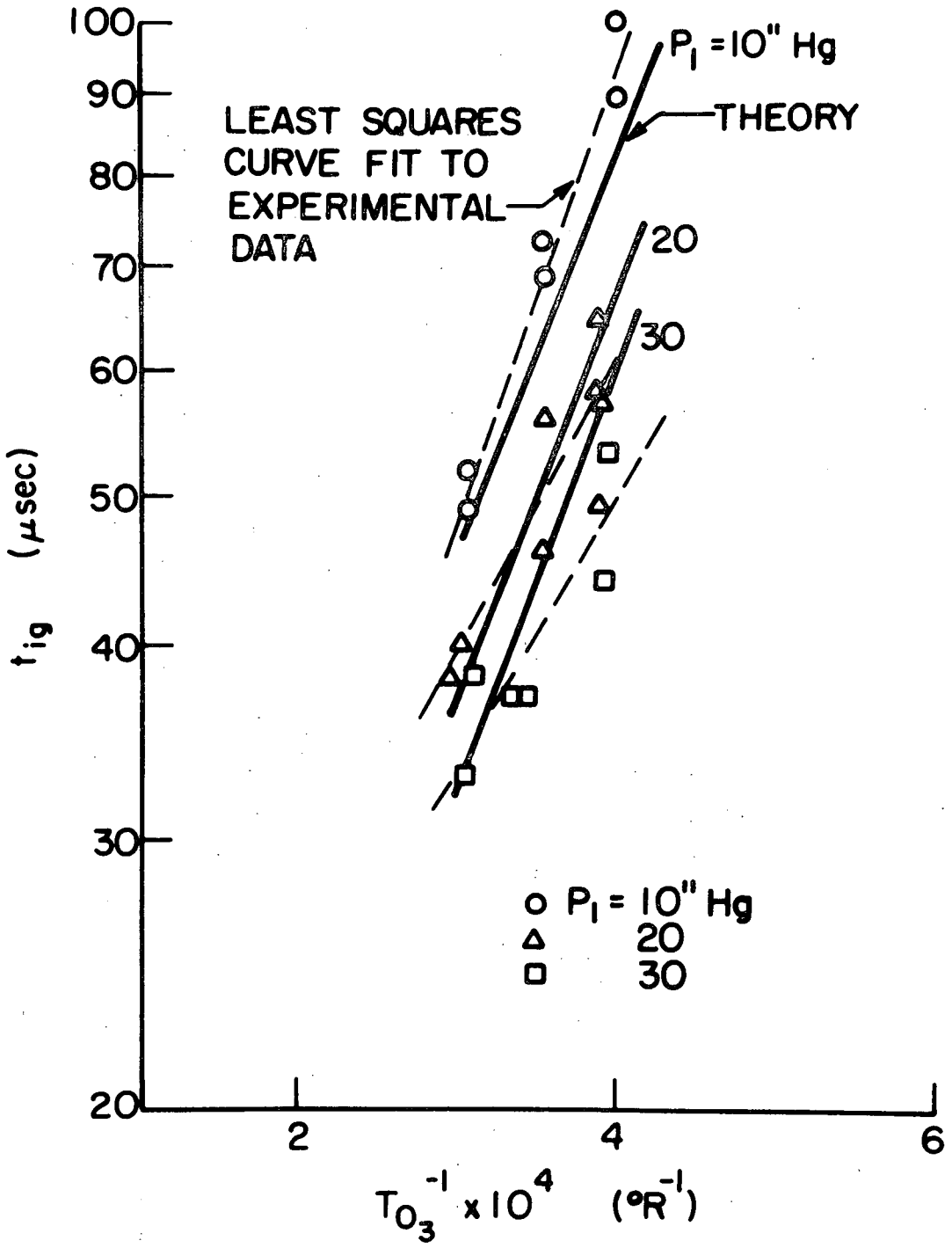

Fig. 19. Comparison of Theoretical Ignition Time with Experimental Data, Single Micromist Droplet Theory; DECH Drops in Pure O_2, $D_O = 930\mu$, $\bar{q}_{v_T} = 7420$ ft-lb/ft^3 (Experimental Data from Ref. 3).

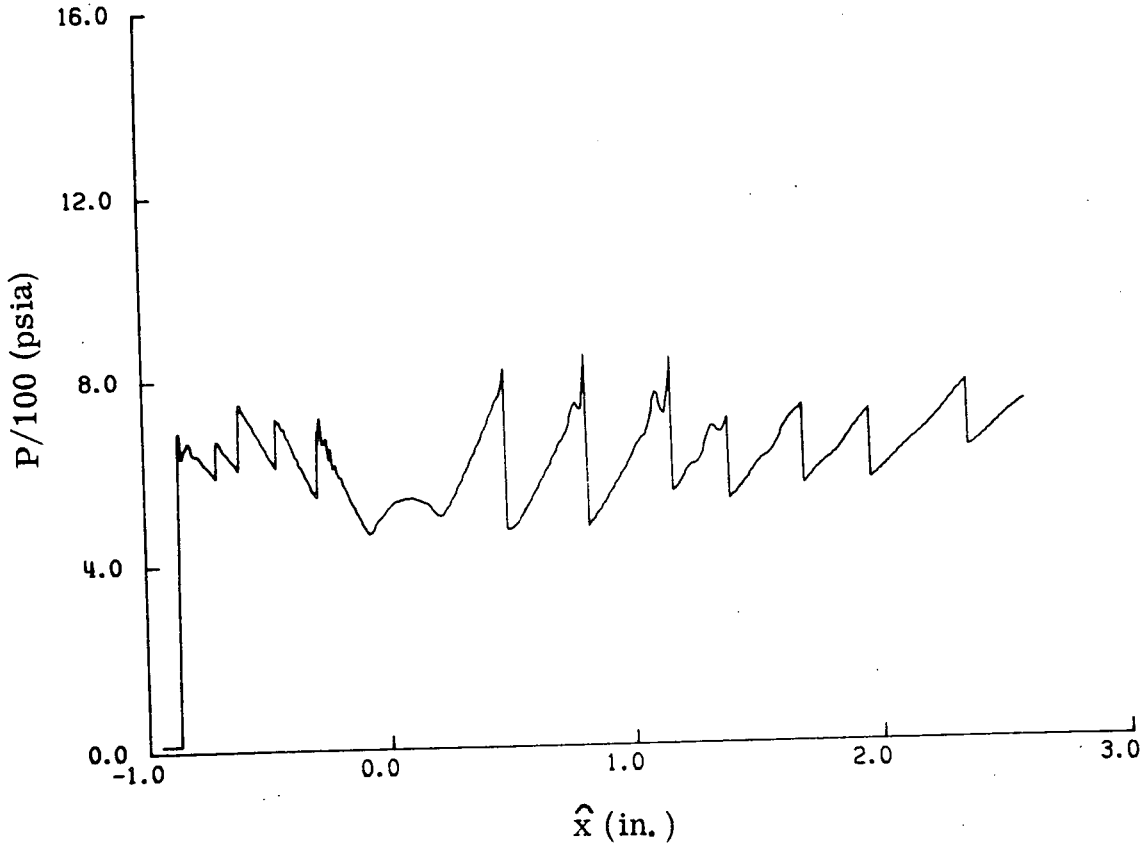

Fig. 20. Theoretical Pressure Distribution from Computer-Animated Film; $\phi = 0.43$, $D_o = 750\mu$, $f = 1.0$; $t = 49.5$ μsec.

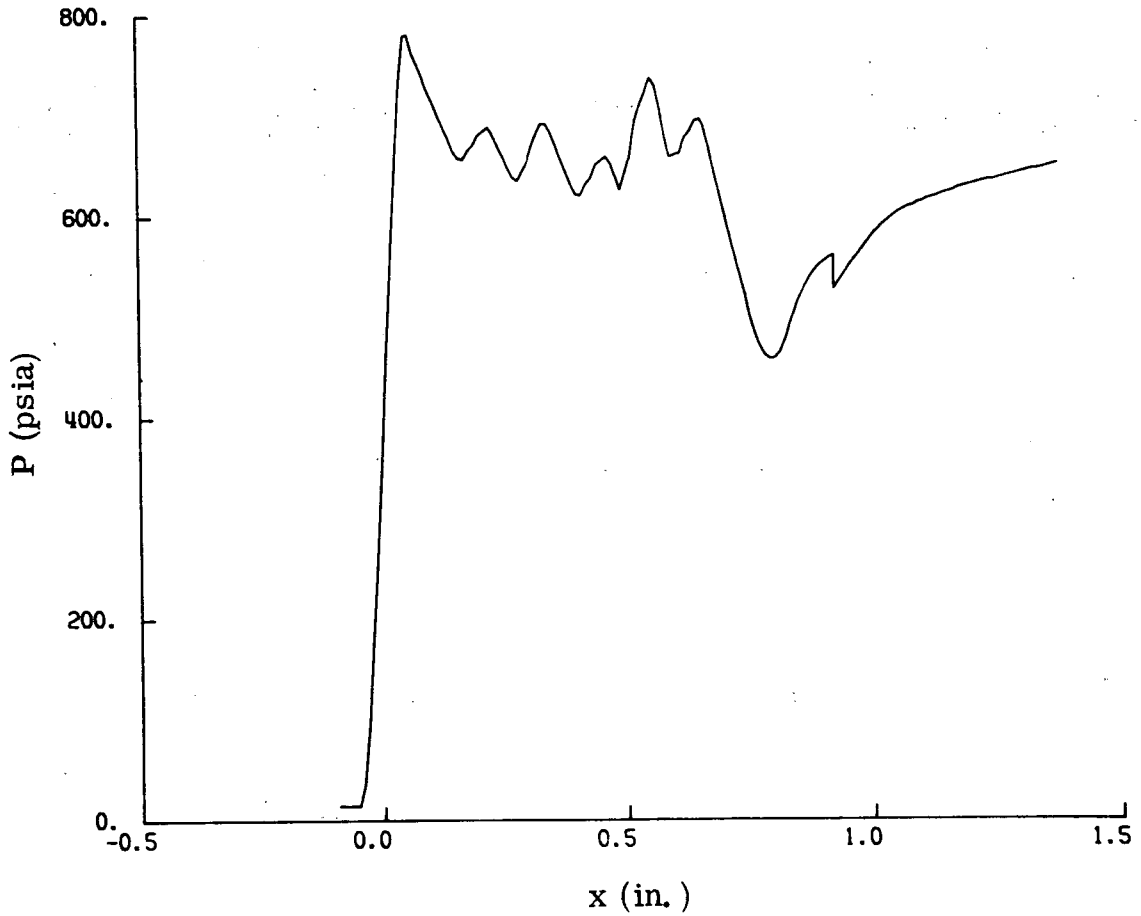

Fig. 21. Pressure Transducer Simulation in Detonation; $\phi = 0.43$, $D_o = 750\mu$, f = 1.0, $\overline{U}_s = 5891$ ft/sec, $R_T = 0.1$ in.

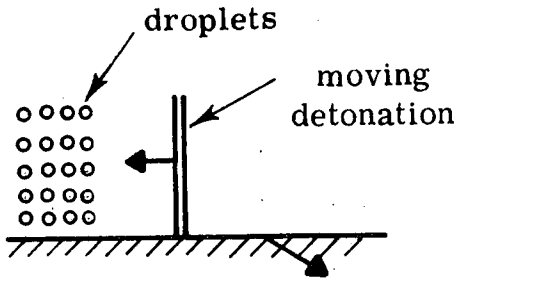

Laboratory Coordinates

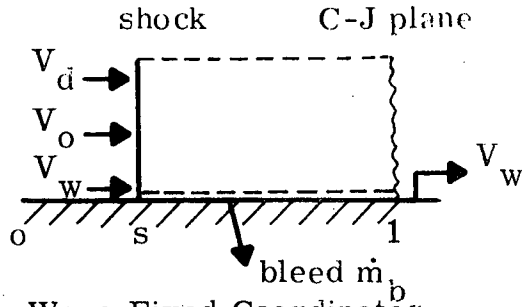

Wave Fixed Coordinates

Notation for Fig. 22-24: $(\ )_o$ - gas, $(\ )_d$ - drops, (1) - behind wave, (s) - shock, (o) - ahead of wave

f = bleed fraction

f_m = fraction of V_s the bleed mass has in leaving C. V.

μ_d = droplet mass flux fraction

$\mu_d = (P_d V_d)/(\rho_o V_o + \rho_d V_d)$

$Q_d^* = (h_d - h_o^o)/(C_P T_o)$ = heat released by droplets

$Q_g^* = (h_o^o - h_1^o)/(C_{P_o} T_o)$ = heat released by gases

m = mean molecular weight

γ = ratio of specific heats

ER = equivalence ratio

$K_d = V_d/V_o$

$P_1^* = P_1/P_o$

$\rho_1^* = \rho_1/\rho_o$

$T_1^* = T_1/T_o$

$M_o = V_o/d_a$

$P_c^* = P_c/P_o$

$T_c^* = T_c/T_o$

$V_w^* = V_w/d_c$

Fig. 22. Jump Conditions for C-J Detonation with Mass Bleed.

2 Phase DECH-O_2 Detonation:

Q_g* 13.340 $\gamma_1 = 1.17$ $\overline{m_1} = 31.32$ $K_d = 1.0$ ER = 0.2

Qd* -8.396 $\gamma_o = 1.40$ $\overline{m_o} = 32.00$ $\mu_d = 0.0552$ $C_{P_o} T_o = 112.08$

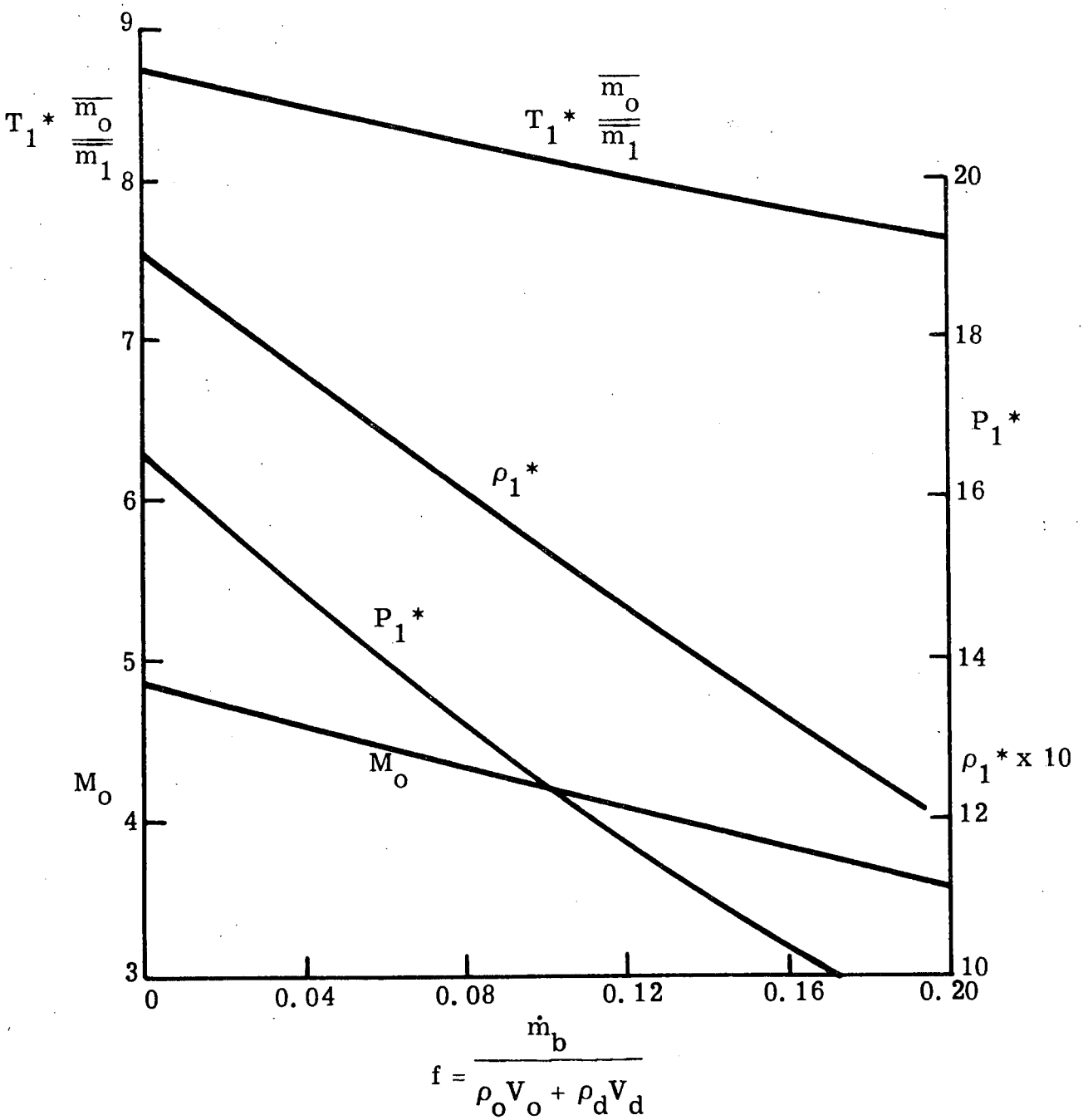

Figure 23. C-J Detonation Wave with Mass Bleed.

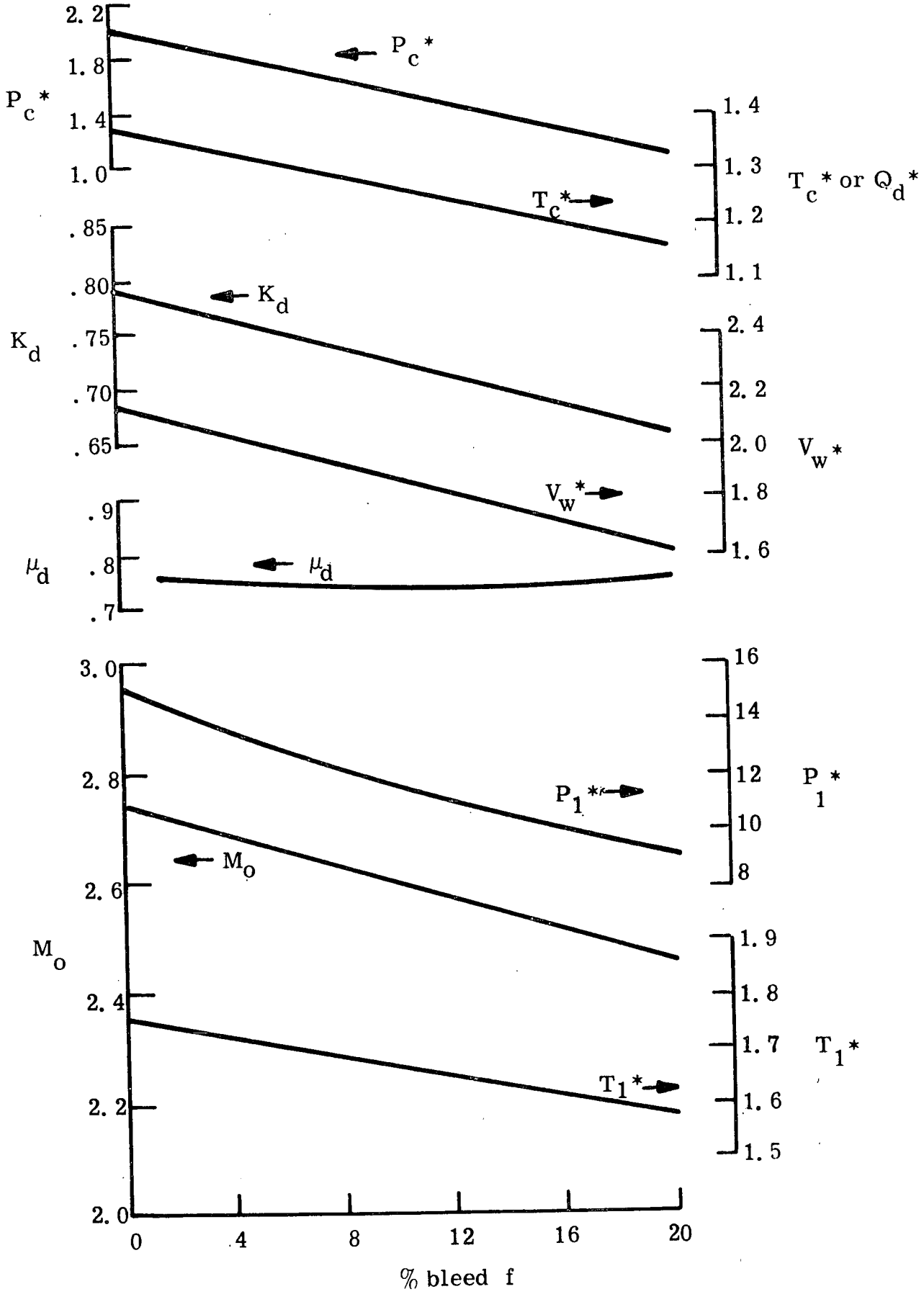

Fig. 24. C-J Detonation Wave with Mass Bleed-Motor Wave.

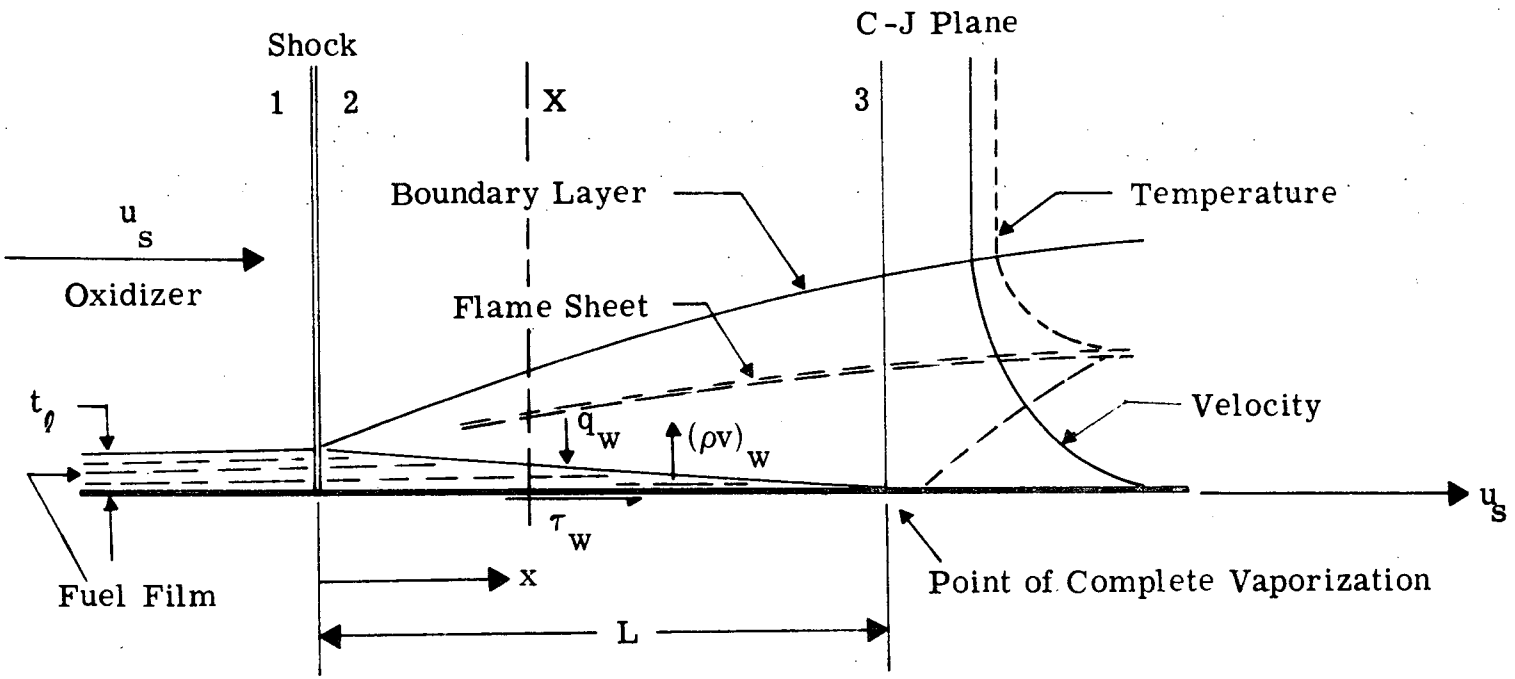

Fig. 25. Two-Dimensional Model for Film Detonations

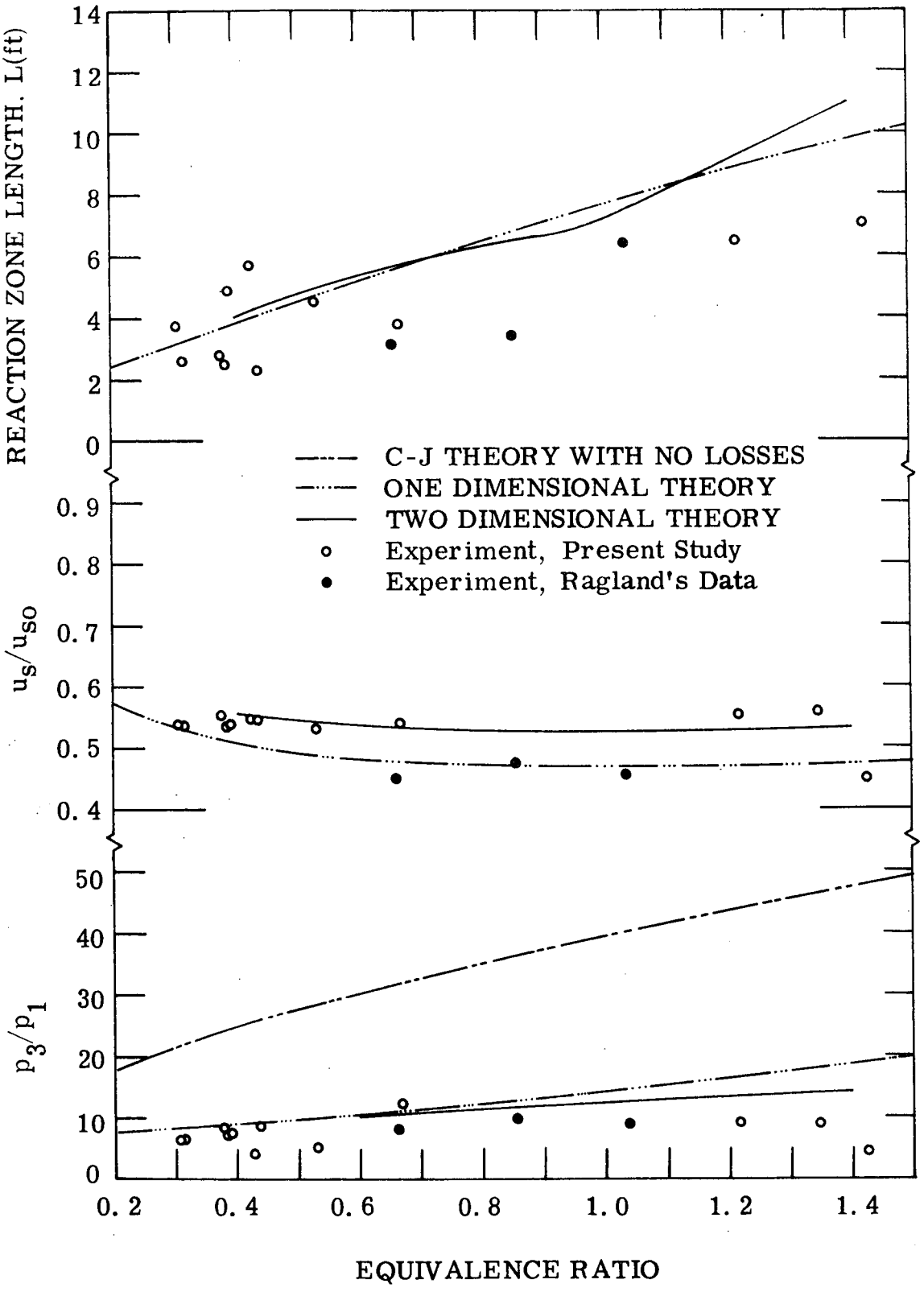

Fig. 26. Propagation Characteristics of One Wall Film Detonations—Comparison of Experiment and Theories
(Fuel - Diethylcyclohexane; Oxidizer - Oxygen)

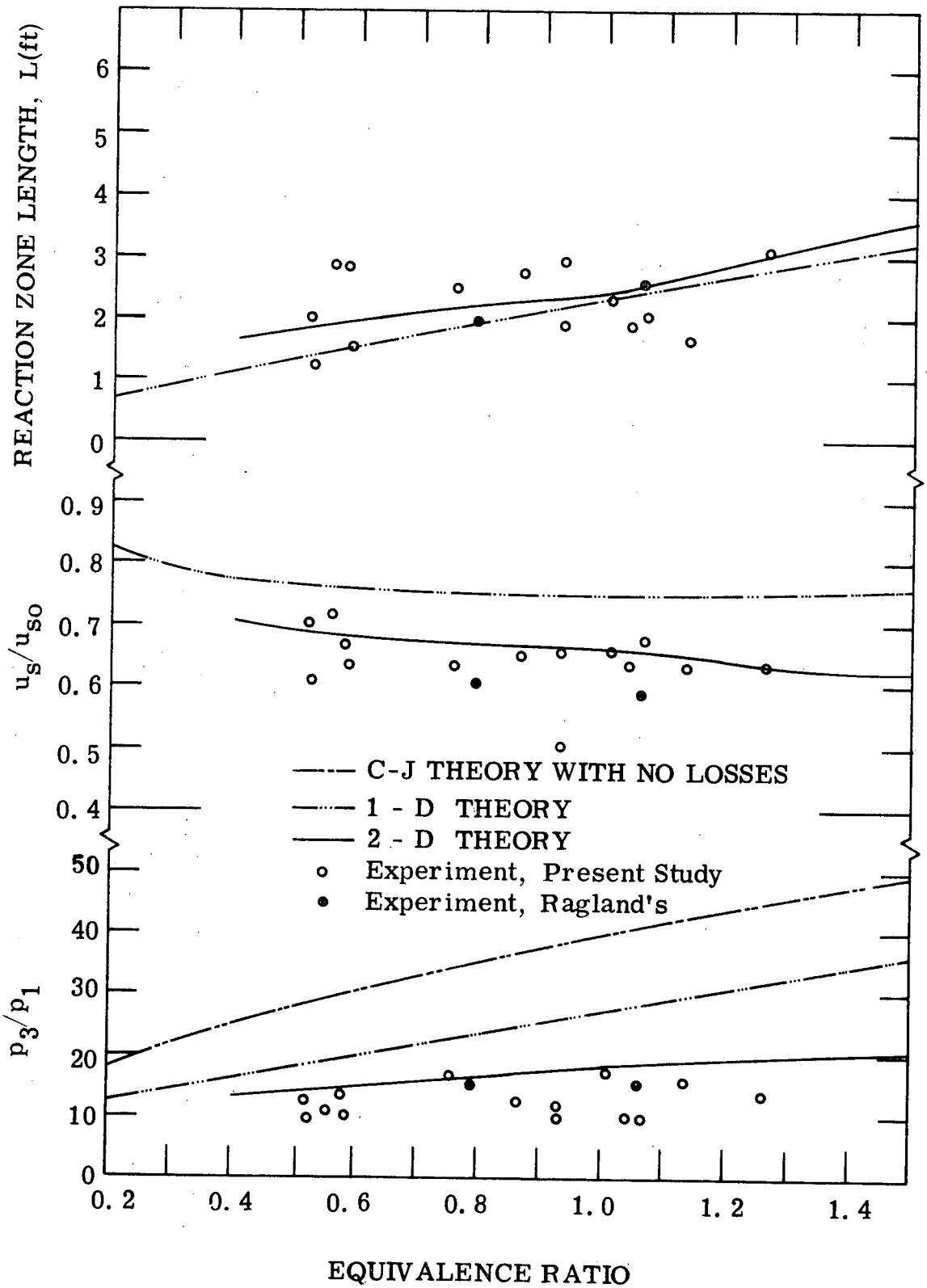

Fig. 27. Propagation Characteristics of Two Wall Film Detonations—Comparison of Experiment and Theories (Fuel - Diethylcyclohexane; Oxidizer - Oxygen)

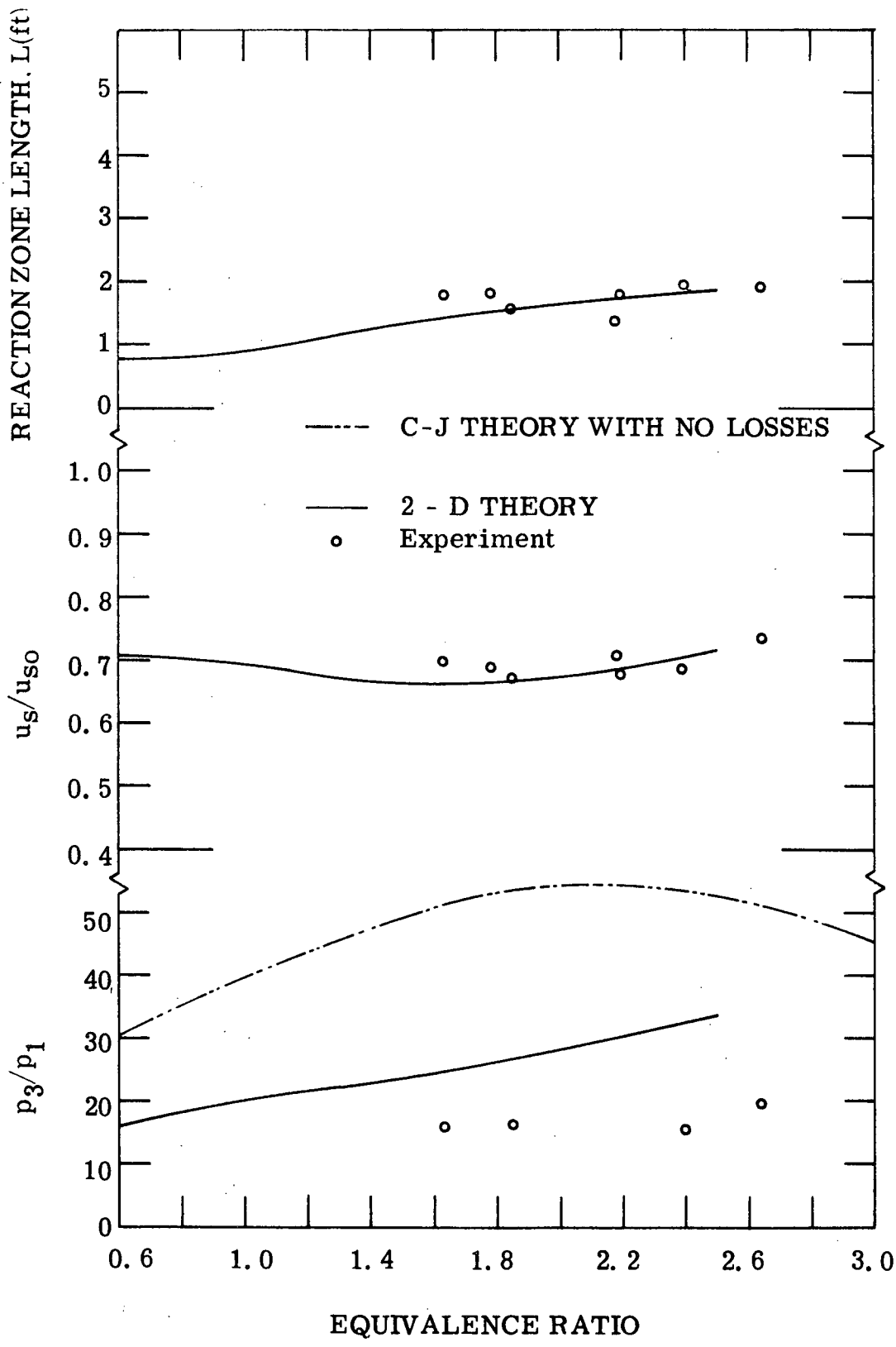

Fig. 28. Propagation Characteristics of Four Wall Film Detonations—Comparison of Experiment and Two-Dimensional Theory (Fuel - Diethylcyclohexane; Oxidizer - Oxygen)

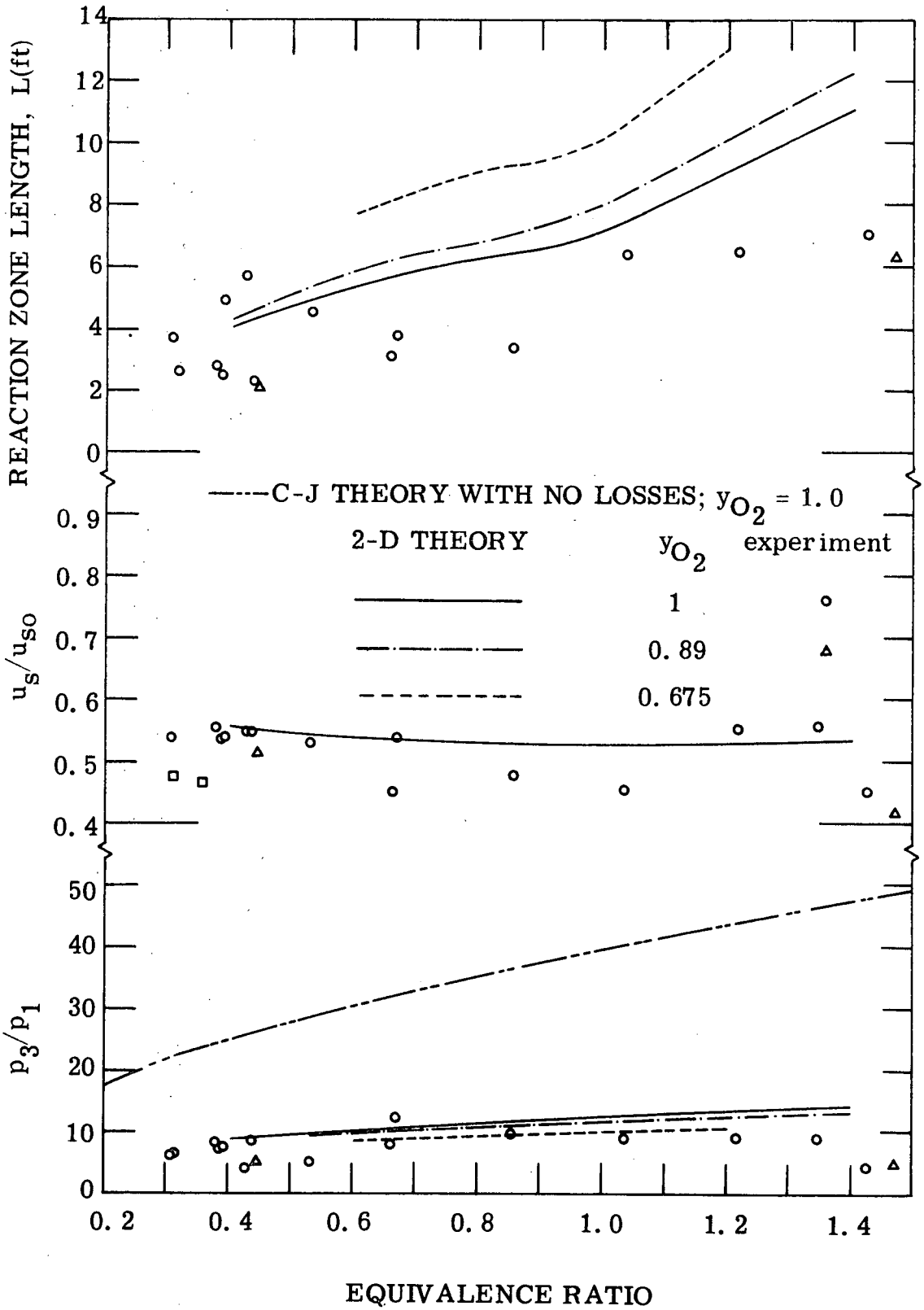

Fig. 29. Effect of Oxidizer Dilution on One Wall Film Detonations—Comparison of Experiment and Two-Dimensional Theory (Fuel - Diethylcyclohexane)

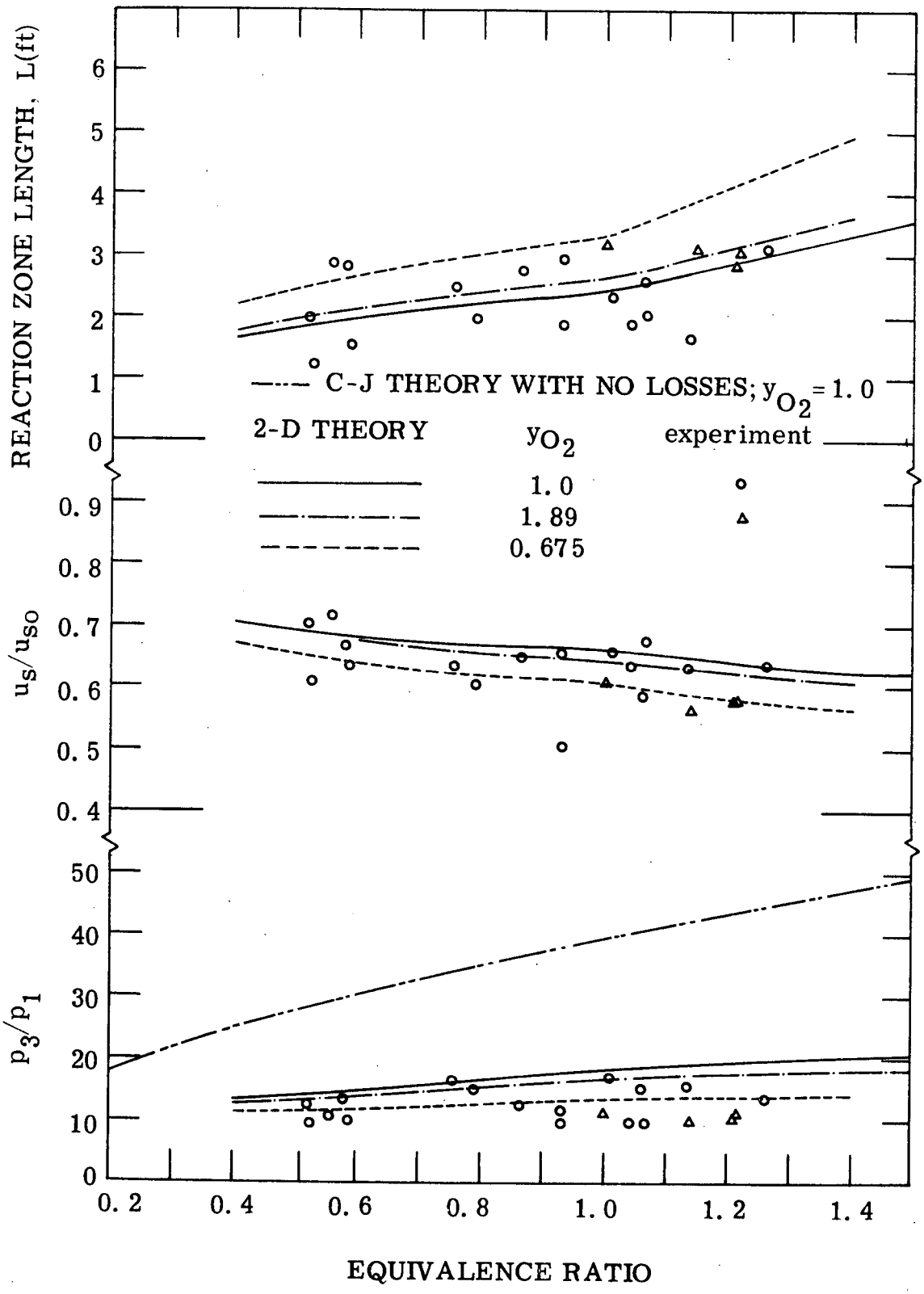

Fig. 30. Effect of Oxidizer Dilution on Two Wall Film Detonations — Comparison of Experiment and Theory (Fuel - Diethylcyclohexane)

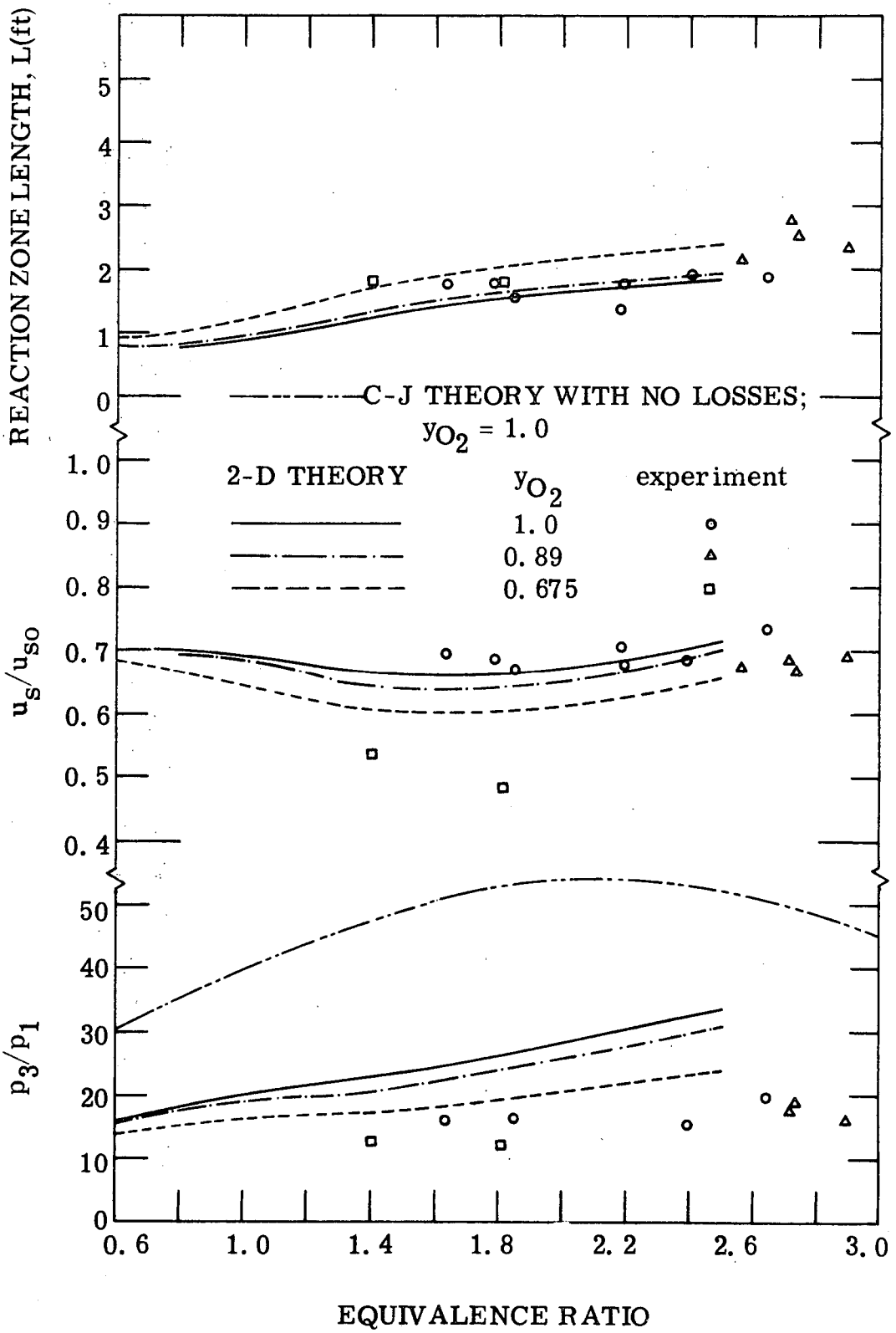

Fig. 31. Effect of Oxidizer Dilution on Four Wall Film Detonations—
Comparison of Experiment and Theory
(Fuel - Diethylcyclohexane)

Dr. R. J. Priem, MS 500-209
NASA Lewis Research Center
21000 Brookpark Road
Cleveland, Ohio 44135 (2)

Norman T. Musial
NASA Lewis Research Center
21000 Brookpark Road
Cleveland, Ohio 44135 (2)

Library
NASA Lewis Research Center
21000 Brookpark Road
Cleveland, Ohio 44135

Report Control Office
NASA Lewis Research Center
21000 Brookpark Road
Cleveland, Ohio 44135

Brooklyn Polytechnic Institute
Attn: V. D. Agosta
Long Island Graduate Center
Route 110
Farmingdale, New York 11735

Chemical Propulsion Information Agency
Johns Hopkins University/APL
Attn: T. W. Christian
8621 Georgia Avenue
Silver Spring, Maryland 20910

North American Rockwell Corp.
Rocketdyne Division
Attn: Paul Combs, D/991-350
Zone 11
6633 Canoga Avenue
Canoga Park, California 91304

National Technical Information Service
Springfield, Virginia 22151 (40)

NASA Representative
NASA Scientific and Technical
Information Facility (2)
P. O. Box 33 (w/Doc Release)
College Park, Maryland 20740

Aerospace Corporation
Attn: O. W. Dykema
Post Office Box 95085
Los Angeles, California 90045

Ohio State University
Department of Aeronautical and
Astronautical Engineering
Attn: R. Edse
Columbus, Ohio 43210

TRW Systems
Attn: G. W. Elverum
One Space Park
Redondo Beach, California 90278

Bell Aerospace Company
Attn: T. F. Ferger
Post Office Box 1
Mail Zone J-81
Buffalo, New York 14205

Pratt and Whitney Aircraft
Florida Research and
Development Center
Attn: G. D. Garrison
Post Office Box 710
West Palm Beach, Florida 33402

Purdue University
School of Mechanical Engineering
Attn: R. Goulard
Lafayette, Indiana 47907

Air Force Office of Scientific Research
Chief Propulsion Division
Attn: Lt. Col. R. W. Haffner (NAE)
1400 Wilson Boulevard
Arlington, Virginia 22209

Pennsylvania State University
Mechanical Engineering Department
Attn: G. M. Faeth
207 Mechanical Engineering Bldg.
University Park, Pennsylvania 16802

University of Illinois
Aeronautics/Astronautic Engineering
Department
Attn: R. A. Strehlow
Transportation Building, Room 101
Urbana, Illinois 61801

NASA
Manned Spacecraft Center
Attn: J. G. Thibadaux
Houston, Texas 77058

Massachusetts Institute of Technology
Department of Mechanical Engineering
Attn: T. Y. Toong
77 Massachusetts Avenue
Cambridge, Massachusetts 02139

Illinois Institute of Technology
Attn: T. P. Torda
Room 200 M. H.
3300 S. Federal Street
Chicago, Illinois 60616

AFRPL
Attn: R. R. Weiss
Edwards, California 93523

U. S. Army Missile Command
AMSMI-RKL, Attn: W. W. Wharton
Redstone Arsenal, Alabama 35808

University of California
Aerospace Engineering Department
Attn: F. A. Williams
Post Office Box 109
LaJolla, California 92037

Georgia Institute of Technology
Aerospace School
Attn: B. T. Zinn
Atlanta, Georgia 30332

Mr. Donald H. Dahlene
U. S. Army Missile Command
Research, Development, Engineering
and Missile Systems Laboratory
Attn: AMSMI-RK
Redstone Arsenal, Alabama 35809

TISIA
Defense Documentation Center
Cameron Station
Building 5
5010 Duke Street
Alexandria, Virginia 22314

Office of Assistant Director
(Chemical Technician)
Office of the Director of Defense
Research and Engineering
Washington, D. C. 20301

D. E. Mock
Advanced Research Projects Agency
Washington, D. C. 20525

Dr. H. K. Doetsch
Arnold Engineering Development Center
Air Force Systems Command
Tullahoma, Tennessee 37389

Library
Air Force Rocket Propulsion
Laboratory (RPR)
Edwards, California 93523

Library
Bureau of Naval Weapons
Department of the Navy
Washington, D. C.

Library
Director (Code 6180)
U. S. Naval Research Laboratory
Washington, D. C. 20390

APRP (Library)
Air Force Aero Propulsion Laboratory
Research and Technology Division
Air Force Systems Command
United States Air Force
Wright-Patterson AFB, Ohio 45433

Technical Information Department
Aeronutronic Division of
Philco Ford Corporation
Ford Road
Newport Beach, California 92663

Library-Documents
Aerospace Corporation
2400 E. El Segundo Boulevard
Los Angeles, California 90045

Princeton University
James Forrestal Campus Library
Attn: D. Harrje
Post Office Box 710
Princeton, New Jersey 08540

U. S. Naval Weapons Center
Attn: T. Inouye, Code 4581
China Lake, California 93555

Office of Naval Research
Navy Department
Attn: R. D. Jackel, 473
Washington, D. C. 20360

Air Force Aero Propulsion Laboratory
Attn: APTC Lt. M. Johnson
Wright Patterson AFB, Ohio 45433

Naval Underwater Systems Center
Energy Conversion Department
Attn: Dr. R. S. Lazar, Code TB 131
Newport, Rhode Island 02840

NASA
Langley Research Center
Attn: R. S. Levine, MS 213
Hampton, Virginia 23365

Aerojet General Corporation
Attn: D. A. Fairchild
Post Office Box 15847
Sacramento, California 95809

Colorado State University
Mechanical Engineering Department
Attn: C. E. Mitchell
Fort Collins, Colorado 80521

University of Wisconsin
Mechanical Engineering Department
Attn: P. S. Myers
1513 University Avenue
Madison, Wisconsin 53706

North American Rockwell Corporation
Rocketdyne Division
Attn: J. A. Nestlerode, AC 46 D/596-121
6633 Canoga Avenue
Canoga Park, California 91304

Tulane University
Attn: J. C. O'Hara
6823 St. Charles Avenue
New Orleans, Louisiana 70118

University of California
Department of Chemical Engineering
Attn: A. K. Oppenheim
6161 Etcheverry Hall
Berkeley, California 94720

Army Ballistics Laboratories
Attn: J. R. Osborn
Aberdeen Proving Ground, Md. 21005

Sacramento State College
School of Engineering
Attn: F. H. Reardon
6000 J. Street
Sacramento, California 95819

Purdue University
School of Mechanical Engineering
Attn: B. A. Reese
Lafayette, Indiana 47907

NASA
George C. Marshall Space Flight Center
Attn: R. J. Richmond, SNE-ASTN-PP
Huntsville, Alabama 35812

Jet Propulsion Laboratory
California Institute of Technology
Attn: J. H. Rupe
4800 Oak Grove Drive
Pasadena, California 91103

University of California
Mechanical Engineering Thermal Sys.
Attn: Prof. R. Sawyer
Berkeley, California 94720

ARL (ARC)
Attn: K. Scheller
Wright Patterson AFB, Ohio 45433

Library
Bell Aerosystems, Inc.
Box 1
Buffalo, New York 14205

Report Library, Room 6A
Battelle Memorial Institute
505 King Avenue
Columbus, Ohio 43201

D. Suichu
General Electric Company
Flight Propulsion
Laboratory Department
Cincinnati, Ohio 45215

Library
Ling-Temco-Vought Corporation
Post Office Box 5907
Dallas, Texas 75222

Marquardt Corporation
16555 Saticoy Street
Box 2013 - South Annex
Van Nuys, California 91409

P. F. Winternitz
New York University
University Heights
New York, New York

I. Forsten
Picatinny Arsenal
Dover, New Jersey 07801

R. Stiff
Propulsion Division
Aerojet-General Corporation
Post Office Box 15847
Sacramento, California 95803

Library, Department 596-306
Rocketdyne Division of Rockwell
North American Rockwell Inc.
6633 Canoga Avenue
Canoga Park, California 91304

Library
Stanford Research Institute
333 Ravenswood Avenue
Menlo Park, California 94025

Library
Susquehanna Corporation
Atlantic Research Division
Shirley Highway and Edsall Road
Alexandria, Virginia 22314

STL Tech. Lib. Doc. Acquisitions
TRW System Group
1 Space Park
Redondo Beach, California 90278

Dr. David Altman
United Aircraft Corporation
United Technology Center
Post Office Box 358
Sunnyvale, California 94088

Library
United Aircraft Corporation
Pratt and Whitney Division
Florida Research and
Development Center
Post Office Box 2691
West Palm Beach, Florida 33402

Library
Air Force Rocket Propulsion
Laboratory (RPM)
Edwards, California 93523

Allan Hribar, Assistant Professor
Post Office Box 5014
Tennessee Technological University
Cookeville, Tennessee 38501

NASA
Lewis Research Center
Attn: E. O. Bourke, MS 500-209
21000 Brookpark Road
Cleveland, Ohio 44135

NASA
Lewis Research Center, MS 500-313
Rockets and Spacecraft
Procurement Section
21000 Brookpark Road
Cleveland, Ohio 44135